AD-A038 824 HONEYWELL INC MINNEAPOLIS MINN SYSTEMS AND RESEARCH --ETC F/G 17/9
MULTICHANNEL INTEGRATED CIRCUIT RADIOMETER DEVELOPMENT.(U)
JUL 75 N00123-74-C-1582

UNCLASSIFIED NL

1 OF 1
AD
A038824

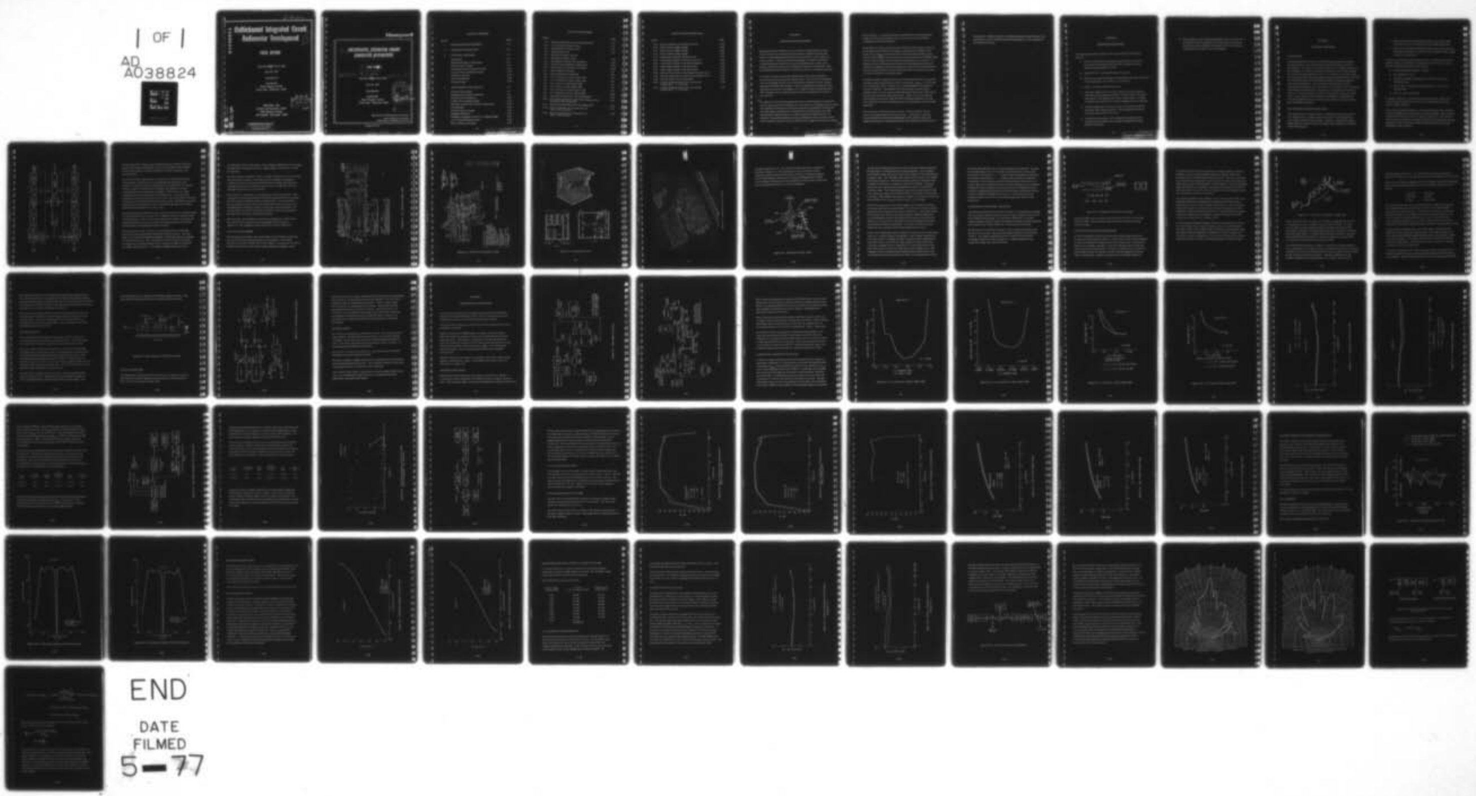

END
DATE
FILMED
5-77

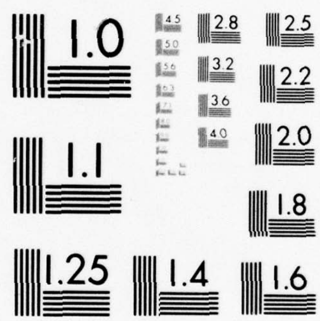

MICROCOPY RESOLUTION TEST CHART
NATIONAL BUREAU OF STANDARDS-1963-A

J. Hooper

ADA038824

Multichannel Integrated Circuit Radiometer Development

1

B. S.

FINAL REPORT

Contract N00~~0~~123-74-C-1582 New

July 18, 1975

Submitted to:

Commander
Naval Weapons Center
China Lake, California 93555

HONEYWELL INC.
Systems and Research Center
2600 Ridgway Parkway
Minneapolis, Minnesota 55413

Reg. # 191459

Honeywell

(6) MULTICHANNEL INTEGRATED CIRCUIT RADIOMETER DEVELOPMENT.

(9) FINAL REPORT.

(15) N00123-74-C-1582

(11) 18 Jul 75

Contract N00123-74-C-1582

(12) 69p.

July 18, 1975

ACCESSION for		
NTIS	White Section	☑
DDC	Buff Section	☐
UNANNOUNCED		☐
JUSTIFICATION Letter on file		
Sheet R77-0310		
DISTRIBUTION/AVAILABILITY CODES		
Dist.	AVAIL. and/or SPECIAL	
A		

Submitted to:

Commander
Naval Weapons Center
China Lake, California 93555

Systems & Research Center
2700 RIDGWAY PARKWAY
MINNEAPOLIS, MINNESOTA 55413

Printed in U.S.A.

402 349

TABLE OF CONTENTS

LIST OF ILLUSTRATIONS

LIST OF ILLUSTRATIONS (Cont.)

SECTION 1

INTRODUCTION AND SUMMARY

Requirements for all-weather ground surveillance capabilities as well as aircraft and missile navigation requirements have initiated considerable interest in developing passive microwave and millimeter wave radiometric sensor systems. Because of the low atmospheric attenuation exhibited at certain frequencies within the microwave-millimeter wave range, such systems show much promise for satisfying all-weather requirements, while possessing sufficient resolution for many surveillance or navigation purposes.

A variety of radiometric system configurations have been developed by government agencies and private industry alike. One of the most intriguing and yet challenging of these is the multichannel radiometric sensor concept developed at NWCCL and elsewhere. Such a multichannel approach promises significant performance advantages over a single-channel scanning approach. The challenge arises in making this type of system competitive in terms of size and cost.

The objective of the present program has been to show feasibility of miniature 35 GHz integrated circuit radiometers for operation in multichannel sensor arrays. The significant achievement of this work has been to successfully demonstrate low noise figure performance for integrated circuit radiometers over large IF bandwidths using miniature, low-cost microstrip circuit structures. In addition, the potential feasibility of large multichannel sensor arrays has been shown using two miniature receiver elements and a single sub-harmonic common

OVER

local oscillator. An equally significant result has been the demonstration of high receiver gain stability for these sensors over video bandwidths extending from 0.01 Hz to 2500 Hz.

Noise figure data taken on the receivers developed in this program approach 6.5 dB (dsb) for 600 MHz IF bandwidths, including IF preamplifier noise figures of 2.5 dB. It is also important to observe that the Schottky diodes used as mixers in these receivers are low cost K_u band devices (HP5082-2769). This is in line with the low cost objectives intended for these receivers. In addition, the use of miniature microstrip circuit techniques and integrated strip-line IF amplifiers and video detectors in this work have shown potential for ultra-miniaturization of receiver elements which is critically important for large multichannel array applications.

Sensitivity of these radiometers in terms of minimum detectable temperature variations at the antenna has been shown to approach $\Delta T_{min} = 2.5°K$ (rms) for a "total power mode" operation over a video bandwidth extending from 0.01 Hz to 2500 Hz. This implies extremely good loss frequency gain stability for the receiver and may ultimately allow "total power mode" operation for these sensors in many applications. Thus, it may be possible to eliminate the necessity for Dicke mode RF switching techniques achieving gain stabilization, thereby simplifying sensor array hardware and increasing sensitivity.

The document is divided into three sections. Section 2 outlines instructions for operating multichannel sensor array. Section 3 is a technical discussion which describes key development areas, problem areas, and design and fabrication considerations which were addressed in the course of

the program. Section 4 provides a detailed description of performance tests conducted on receiver elements operated individually as well as together in the multichannel array.

SECTION 2

OPERATING INSTRUCTIONS

The following procedure should be used for operating the multichannel receiver.

1. Check to see that the RF waveguide inputs to each receiver are clean and free of foreign material before making connections. (Tapped waveguide holes are 4-40.)

2. Apply +28 V.D.C. at approximately 0.3 amperes.

3. Check to see if proper voltages are being delivered to the electronics via the test points. ($\pm$ 15 V.D.C., +7.5 V.D.C.)

4. Allow a 15 minute stabilization period.

5. The video output from each receiver appears at their respective OSM connectors on top of the chassis. Caution must be exercised not to place a DC voltage on the receiver video output. A change in detector bias could result, thereby changing receiver sensitivity.

6. The gain adjustments for each receiver are located immediately behind the video output connector. The pots adjust the receiver attenuator between 0 and -10 V.D.C.

7. The Gunn local oscillator can be adjusted in frequency by the mechanical screw which can be seen by removing the left side panel of the chassis.

8. The DC block is used in the local oscillator coax to receiver No. 1. DC isolation must be provided between each receiver to prevent the self bias of the multiplier in receiver No. 1 from interfering with the bias of the other receiver's multiplier.

SECTION 3

TECHNICAL DISCUSSION

INTRODUCTION

The following technical discussion describes key development activities including problem areas which have been addressed during the course of this program. The result of this work has been to successfully demonstrate the feasibility of a 35 GHz multichannel radiometric sensor array utilizing low cost microstrip integrated circuits. The radiometric receivers which were developed exhibit noise figure performance approaching 6.5 dB (dsb with 2.5 dB IF noise figure) over broad RF bandwidths with good potential for even lower noise figures. The microstrip circuit design has further demonstrated potential for ultra-miniaturization of these receivers especially when utilized in multichannel configurations. As total power radiometers, these I.C. sensors have proven to have extremely good ΔT_{min} sensitivity on the order of 3°K for video bandwidths extending from .01 to 2500 Hz. For some applications this may eliminate the need for conventional Dicke gain stabilization techniques.

MULTICHANNEL SENSOR ORGANIZATION

The multichannel or "staring" sensor system offers improved sensitivity over single channel scanning systems due to the increased integration time available with this type of design. However, a multichannel system organization also imposes several challenges to the designer as indicated on the following page.

- Since several receiver channels are used, each receiver must be small in order to meet overall size and weight constraints.
- Since several receiver channels are used, each receiver must be relatively inexpensive in order to be cost competitive with a single channel scanning system.

In order to meet nominal performance goals for a multichannel midcourse guidance sensor, each individual radiometric sensor in the array must meet the following performance requirements:

- Nominal operating frequency = 35 GHz.
- RF bandwidth ≥ 1 GHz.
- Minimum detectable sensitivity of 0.25°K or less with 1 sec integration time.
- RF-to-video transfer gain of 90 dB level to ± 3 dB over the RF bandwidth.
- Dynamic range of 50-60 dB.

In addition radiometric receiver elements should each be smaller than 2 cubic inches and weigh less than 8 ounces with potential for further size and weight reduction.

In the present feasibility program, a three-channel radiometric receiver array was developed with two receiver channels populated. The functional organization of the array system is shown in Figure 3-1. This receiver array has been designed as a concept feasibility unit for laboratory testing purposes in order to demonstrate viable radiometer performance with integrated circuit structures.

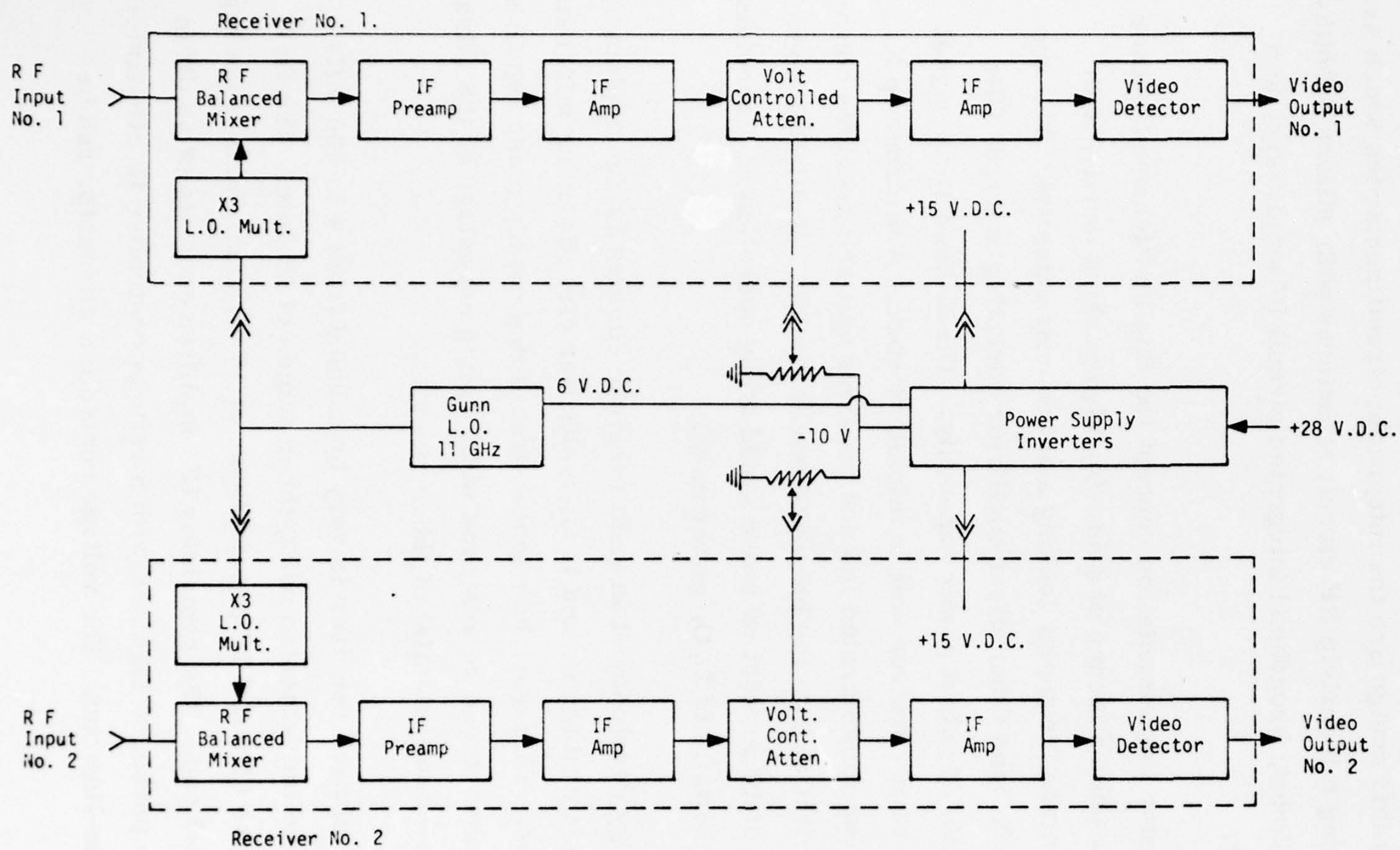

Figure 3-1. Multichannel System Functional Organization

Key elements in this design are the integrated circuit receivers which are implemented using microstrip RF circuit structures with silicon Schottky barrier mixer diodes, broadband integrated circuit IF amplifiers, and a video detector.

The local oscillator implementation concept for this multichannel sensor array provides a unique means of achieving high packing density with receiver-to-receiver frequency locking and low cost potential. The concept utilizes a single X-band Gunn effect oscillator operating at 11.67 GHz with 200 milliwatts of output power capability. The X-band L.O. signal is distributed to each receiver unit in miniature coax. A microstrip X3 multiplier has been implemented in each receiver unit and provides conversion to K_a band for injection into the balanced mixer circuit. Multiplier conversion efficiency goals of 10 percent or more would allow operation of 5 receiver elements of 4 milliwatts of L.O. power each.

The key technology development in each receiver element is the implementation of both the RF balanced mixer and L.O. multiplier circuits using microstrip circuit techniques. This work has demonstrated that usable noise figure and bandwidth performance can be achieved while taking advantage of the ultra small size and low cost potential of these circuits.

The IF assembly of each receiver is very broadband from 4 to 600 MHz (3 dB) and has been implemented using three stages of IF gain. The first stage is a low noise (2.5 dB) IF preamplifier of 16 dB gain which is packaged in a standard TO-8 can. The remaining IF amplifier consists of 56 dB in two stages and is packaged together with a voltage controller IF attenuator in a single dual-in-line can. The voltage controlled attenuator can be

varied between 0 and -16 dB using a control voltage ranging from 0 to -10 volts. The entire IF assembly operates on a supply voltage of +15 V.D.C. at about 85 milliamps.

The video detector consists of a silicon Schottky diode which is forward biased with about 100 microamps. The video detector assembly is packaged in a small 1/2 inch by 1/4 inch by 1/8 inch flat-pack complete with impedance matching circuits for IF matching to 50 ohms over 1 to 600 MHz and video matching to 300 ohms over 0 to 1.2 MHz.

Each receiver is mounted in a brass package as shown in Figure 3-2. This represents a convenient package for feasibility testing purposes but certainly does not represent ultimate receiver miniaturization. It is conceivable that the packaged receiver size can be reduced by a factor of 5 or more by integrating the IF and video circuitry on to the microstrip substrates. As shown in Figure 3-3 the IF and video assemblies consist of conventionally packaged ICs mounted on a printed circuit board.

Both receivers, local oscillator, and power conditioning assemblies have been mounted into a multichannel array package which is shown in Figure 3-4. The individual receiver element is shown in Figure 3-5.

BALANCED MIXER DESIGN

The development of a planar microstrip balanced mixer with low conversion loss is one of the key accomplishments in this program. The critical elements of the mixer include a 90° branch coupler, a matched pair of silicon Schottky barrier mixer diodes with suitable impedance mounting, and an

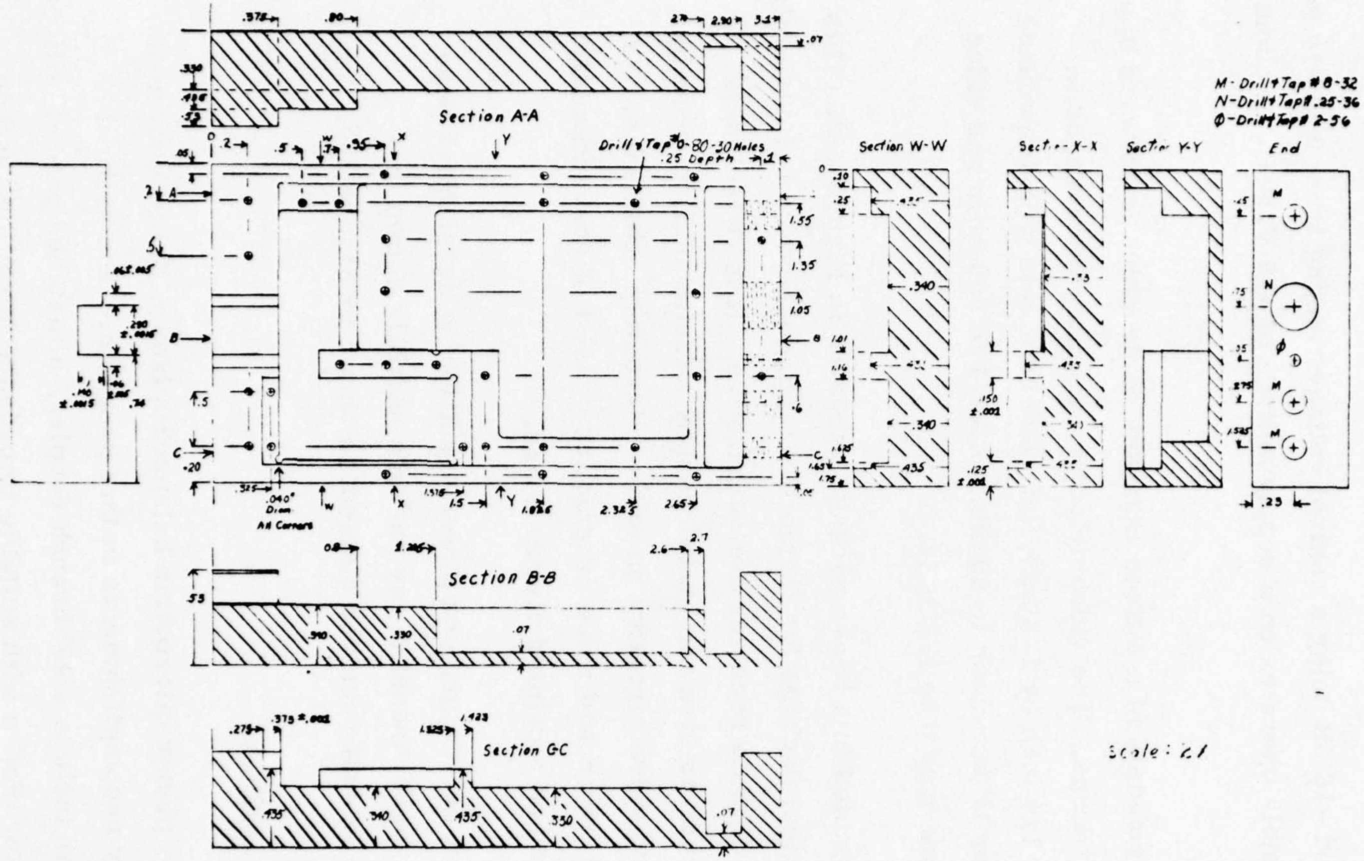

Figure 3-2. I.C. Receiver Package Layout

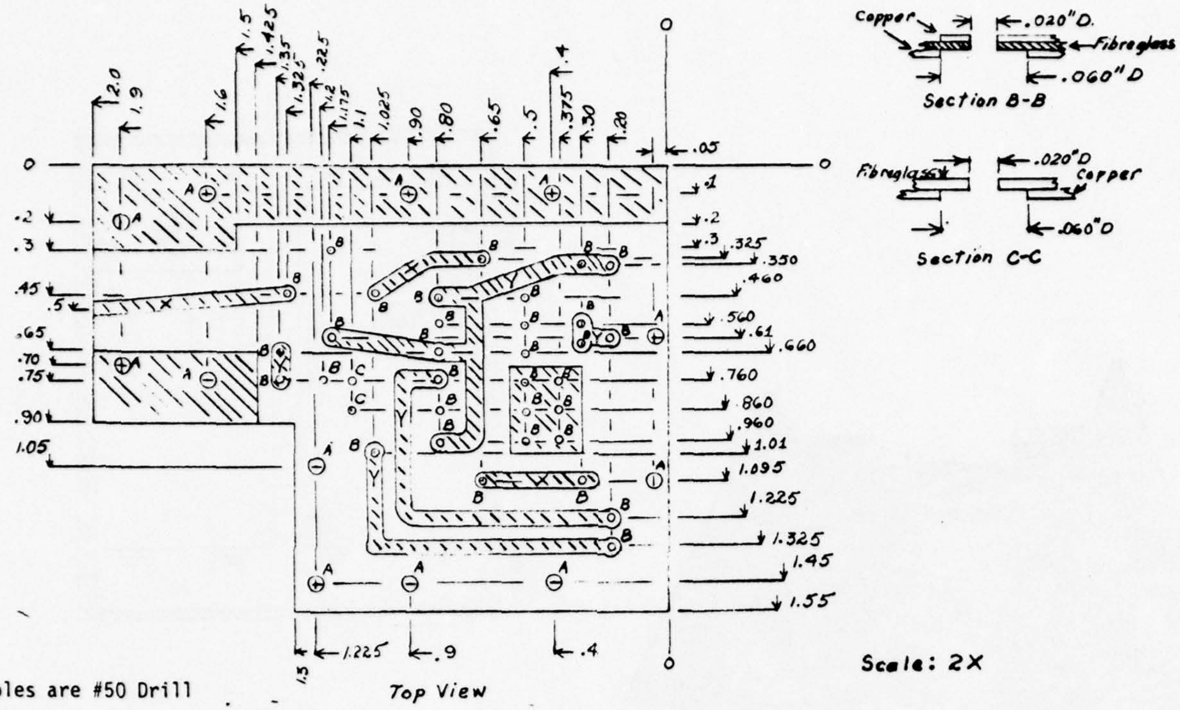

1. A holes are #50 Drill
2. B holes are #75 Drill. Holes under connecting straps are as shown in Section B-B except for 6 holes under the rectangular Grounding Pad which are drilled straight through to permit soldering to ground plane.
3. C holes are #75 Drill See Section C-C
4. Copper not removed from board bottom except for hole clearance
5. X straps are .080" wide
6. Y straps are .050" or less as is convenient

Material: .032" Double Copper Clad Epoxy-Fiberglass

I.C. Receiver P.C. Bd.
Honeywell SRC
J.K. 3/4/75
Ext. 5309

Figure 3-3. IF/Video Circuit Board Layout

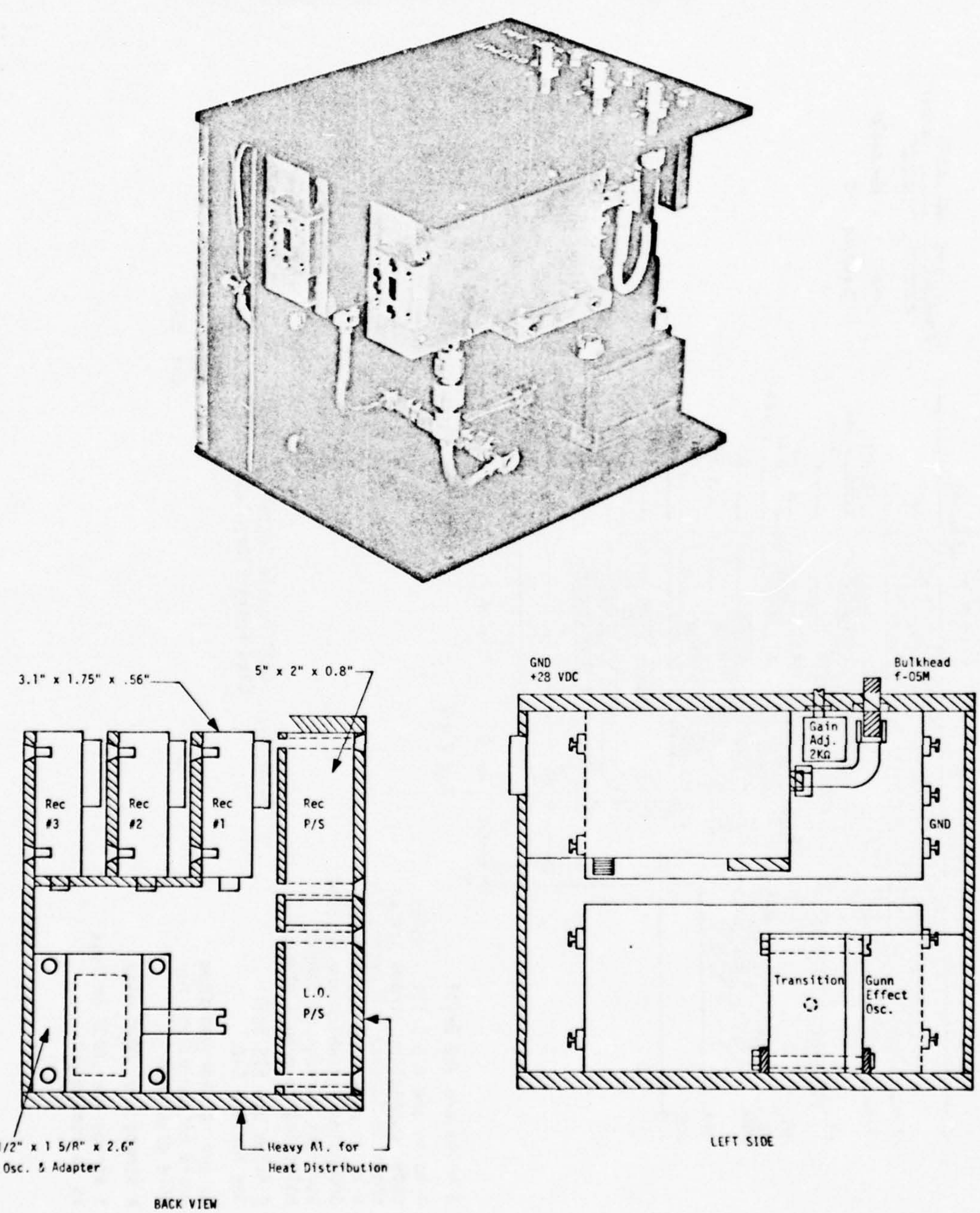

Figure 3-4. Multichannel Array

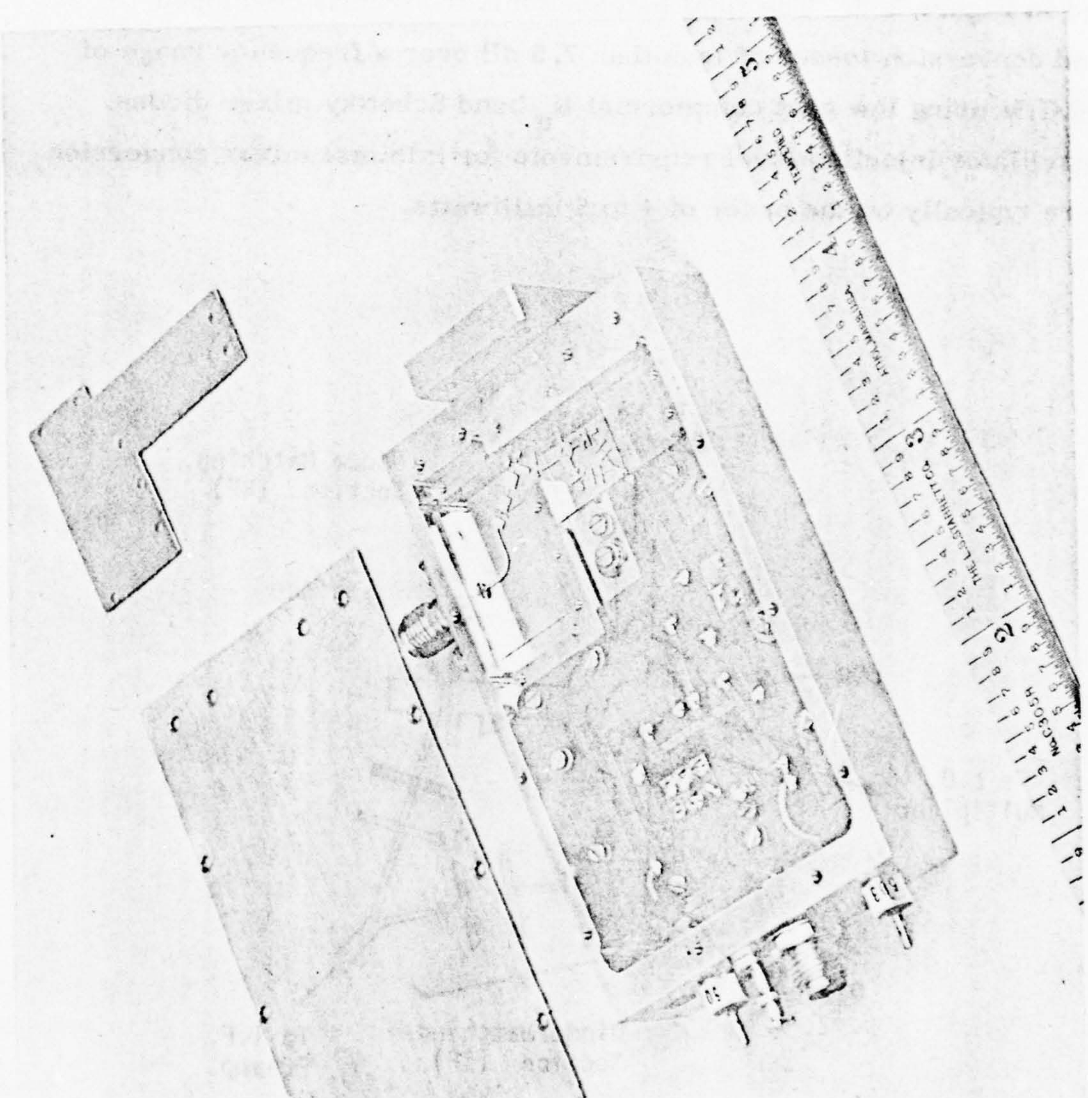

Figure 3-5. Individual Receiver Element

IF output coupling circuit. The layout of the balanced mixer assembly is included in Figure 3-6. The final balanced mixer circuits developed exhibited conversion losses of less than 7.5 dB over a frequency range of 32 to 36 GHz using low cost commercial K_u-band Schottky mixer diodes. Local oscillator injection level requirements for minimal mixer conversion loss were typically on the order of 4 to 6 milliwatts.

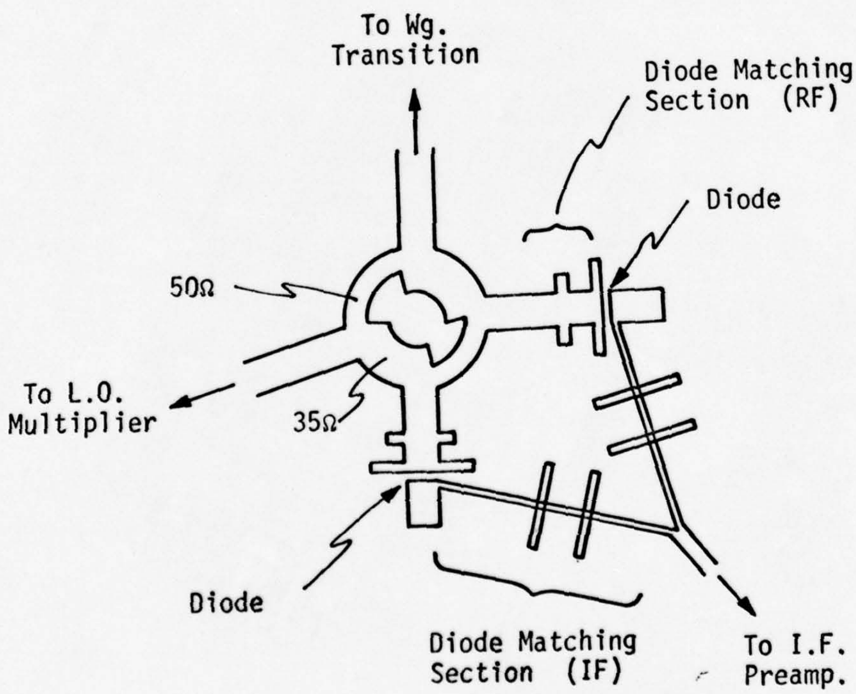

Figure 3-6. RF Balanced Mixer Layout

The 90° branch coupler consists of a circular microstrip ring to which all RF input lines are designed to be of 50 ohm impedance. To accomplish the 3 dB power split, two quarter-wave branch legs were used with 50 ohms impedance each. The main legs in the ring are also of quarter wavelength with 35 ohm impedance. The branch coupler provides a 3 dB power split to within $\pm$ 0.85 dB over a frequency range of 32 to 38 GHz. The power split for the two input ports is symmetrical to within 0.2 dB over this frequency range. The isolation between input ports is greater than 15 dB over a frequency range of 32 to 38 GHz and has a maximum value of 30 dB at 35 GHz. Input VSWR to the 90° branch coupler is less than 1.7:1 between 32 and 38 GHz with a minimum value of about 1.1:1 at 35 GHz.

The 50 ohm output ports of the branch coupler are matched to the mixer diode input impedance of approximately 10 + j 12 ohms at 35 GHz using the lumped element matching section shown in Figure 3-6. The diodes used in the balanced mixer were low cost K_u-band diodes (HP5082-2769) which were individually matched on the basis of RF impedance and conversion efficiency as measured in a standardized microstrip single-ended mixer configuration developed by Honeywell. The diodes were of beam-lead design and were mounted using a thermocompression process.

In the circuit configuration shown in Figure 3-6 the mixer were self-biased with a d.c. current of about 2.0 milliamps. The IF output impedance of each mixer diode is nominally 200 ohms, and the parallel combination of both diodes yields a net mixer IF output impedance of about 100 ohms. A low-pass coupling circuit is implemented in microstrip between each mixer diode and the common IF output point shown in Figure 3-6. This coupling circuit is a lumped element implementation which allows each mixer diode to view the IF circuit at 35 GHz as a load impedance element

of greater than 200 ohms over a frequency range of 30 to 40 GHz. Thus the IF assembly appears as a relative open-circuit to the mixer diode at RF frequencies. In initial circuit designs the mixer IF impedance of 100 ohms was matched to the 50 ohm IF preamplifier using a broadband impedance transformer. Since the insertion loss of the impedance transformer was nearly 1 dB, it was eliminated in favor of direct coupling to the preamplifier. Although the obvious impedance mismatch reduces IF coupling efficiency, the direct coupling provided better overall noise figure performance for the receiver and better bandwidth characteristics. In future units IF preamplifiers will be used which are specially designed for 100 ohm input impedances.

WAVEGUIDE-TO-MICROSTRIP TRANSITION

A broadband waveguide-to-microstrip transition was developed for providing efficient energy coupling between the incident TE_{10} waveguide mode and the quasi-TEM microstrip mode. The transition consisted of a 4-section stepped-ridgeline structure which was designed to provide a 4-pole Chebychev type response with minimal VSWR over a passband of 32 to 38 GHz.

The RF input port was RG-96 waveguide, and an input mode impedance of 472 ohms was assumed. The microstrip output impedance was nominally 50 ohms. The stepped-ridgeline transition consisted of four quarter wavelength sections as shown in Figure 3-7. Ridge impedances were designed to be 410, 234, 101 and 58 ohms.

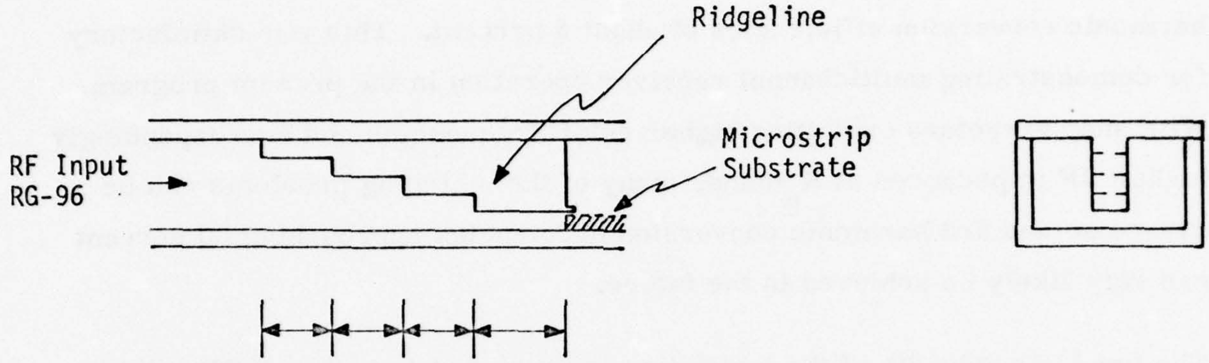

Figure 3-7. Waveguide-to-Microstrip Transition

Measured VSWR on the transitions were less than 1.17:1 over a bandwidth of 33 to 36 GHz. Insertion losses were less than 0.7 dB over the same frequency range.

LOCAL OSCILLATOR MULTIPLIER DESIGN

In order to provide X-band to K_a-band local oscillator signal conversion for injection into the balanced mixers, a third harmonic microstrip multiplier circuit was developed for integration into each receiver unit. Performance goals for the multiplier included a conversion efficiency goal of 10 percent using a snap-varactor type diode. A number of problems were encountered in providing a proper RF impedance match to the low impedance varactor diode, and ultimately a parallel combination of two Schottky diodes was

selected because of the reduced impedance matching problem. The final multiplier circuits utilizing Schottky diodes were able to achieve 3rd harmonic conversion efficiencies of about 5 percent. This was satisfactory for demonstrating multichannel receiver operation in the present program. With snap varactors exhibiting higher cutoff frequencies and correspondingly higher RF impedances at K_a-band, many of the matching problems can be overcome and 3rd harmonic conversion efficiencies approaching 30 percent can very likely be achieved in the future.

The tunable bandwidth of the multiplier is somewhat less than 2 GHz and is primarily defined by the bandpass characteristics of the 3rd harmonic output filter as well as diode matching considerations. Direct coupling of fundamental frequency components between input and output ports of the multiplier is suppressed by more than 40 dB. Similarly 35 GHz frequency components appearing at the multiplier input port are suppressed with respect to the output port by more than 30 dB.

The 3rd harmonic multiplier design consists of a low-pass filter section for X-band signal input, a diode mounting section, a second harmonic resonator section, and a bandpass filter section for K_a-band signal output. The layout of the final multiplier configuration is shown in Figure 3-8. The entire circuit is configured on a 3/4 inch by 1/2 inch quarts substrate using chrome-gold conductors and pholoIithographic circuit fabrication.

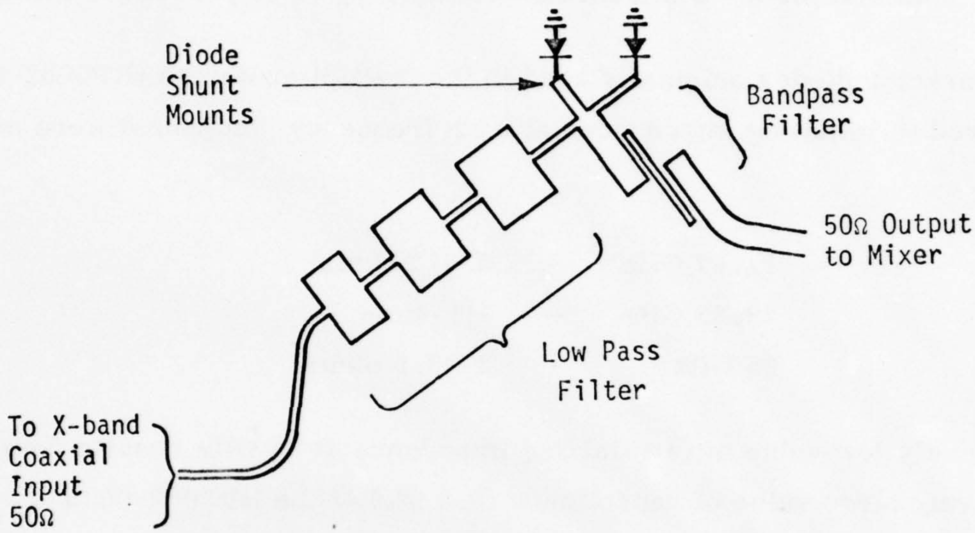

Figure 3-8. 3rd Harmonic Multiplier Configuration

In this circuit X-band L.O. signal at 11.67 GHz is supplied to the receiver via miniature coax and a simple transition to 50Ω microstrip. An input low pass filter provides proper impedance matching to the diodes at the fundamental frequency and suitably isolates the input circuit from harmonics generated by the diodes. A fundamental impedance of 10 ohms is required by the Schottky diode combination. The low pass filter has a 3 dB rolloff at 13 GHz and an insertion loss of less than 1.0 dB.

The Schottky diodes perform as nonlinear resistors to provide multiplication. Because they are resistive and consume power themselves, the Schottky multipliers tend to be less efficient than the varactors which are theoretically purely reactive and consume no power. Theoretical efficiency for the Schottky multipliers goes approximately as n^{-2} where n in the order of

multiplication (in this case n = 3). Efficiency for the varactors ideally goes as n^{-1} so that for n = 3 a theoretical efficiency of 33 percent is achievable.

For the varactor diodes originally used in the multiplier design (HP5082-0008), the required terminating impedances at each frequency component were as follows:

11.67 GHz	-	5 -j10 ohms
23.33 GHz	-	-j5 ohms
35 GHz	-	2 -j3.5 ohms

The extremely low value of terminating impedance at 35 GHz results from the relatively large value of capacitance (0.5 pf.) of the HP5082-0008 varactor diode at this frequency. This impedance proved to be extremely difficult to match, and the quality of the match was very sensitive to any stray reactances associated with the diode mount. Several different shunt mounting configurations were tried but well behaved, reproducible impedance matches to the diode at 35 GHz could not be satisfactorily achieved.

Improved diodes exhibiting lower capacitance (higher cutoff frequency) and larger values of K_a-band impedance were not readily available. For this reason it was decided to utilize Schottky diodes and accept the reduced conversion efficiency. The diodes selected were Aertech No. A25781 in beam lead configuration. The diodes do not utilize external d.c. biasing in the present circuit configuration.

In the final multiplier circuit shown in Figure 3-8 the diode impedance at the 2nd harmonic frequency is suitably matched using a resonator circuit at 23.33 GHz. This resonator primarily consists of a quarter wave 50 ohm

line which also serves as an input line to the 3rd harmonic bandpass filter. This short section of line is terminated by the diode combination on one end and on the opposite end by an approximate open circuit as observed at 23.3 GHz. Since the line is nominally a quarter-wave long at the 2nd harmonic frequency, it appears as a near short to the diode as required.

The 3rd harmonic bandpass filter section consists basically of a half-wave resonator shown in Figure 3-8 which is edge-coupled to the adjacent input and output lines. The 3 dB roll-off points for the bandpass filter are approximately at 33.8 GHz and 36.2 GHz. The insertion loss of the filter at 35 GHz is no more than 1.2 dB.

IF/VIDEO ASSEMBLY

The complete IF/video assembly is mounted on a double clad printed circuit board with one side acting as the ground plane. The circuit board is mounted to the housing via mounting screws around its perimeter.

The mixer output is bonded to the input of an Avanteck UTO-511 (16 dB) preamplifier via a small copper strap. The preamplifier is followed by an Avanteck SDP-8278 amplifier/attenuator as shown in Figure 3-9. This package has adjustable gain from about 39 to 56 dB. The attenuator is controlled via 0 to -10 V.D.C. (2 ma max.) signal supplied through a ferrite bead and an RFI filter mounted on the case. The +15 V.D.C. power is also supplied through an RFI filter and ferrite bead.

The output of the amplifier/attenuator feeds a Schottky diode MA-7707J acting as video detector. The detector is forward biased with 100μa of current supplied through a 150 kΩ resistor to the +15 volt supply. The

detector output is d. c. coupled to the OSM video output connector. The video detector output impedance will nominally be about 300 ohms.

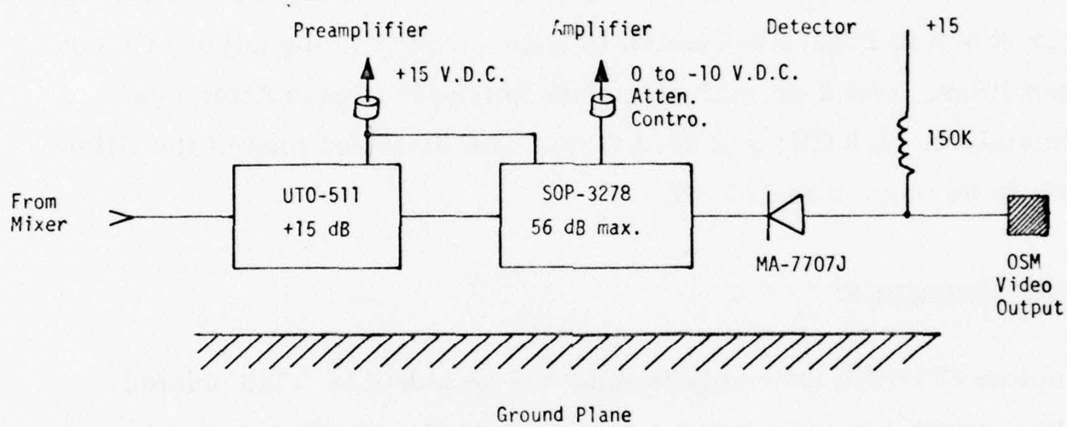

Figure 3-9. Block Diagram of IF/Video Assembly

POWER CONDITIONING

The multichannel radiometer requires -28 V. D. C. at about 0. 3 amperes. Two DC/DC converters supply the necessary power to the electronics (+15, -15, +7. 5) as shown in Figure 3-10.

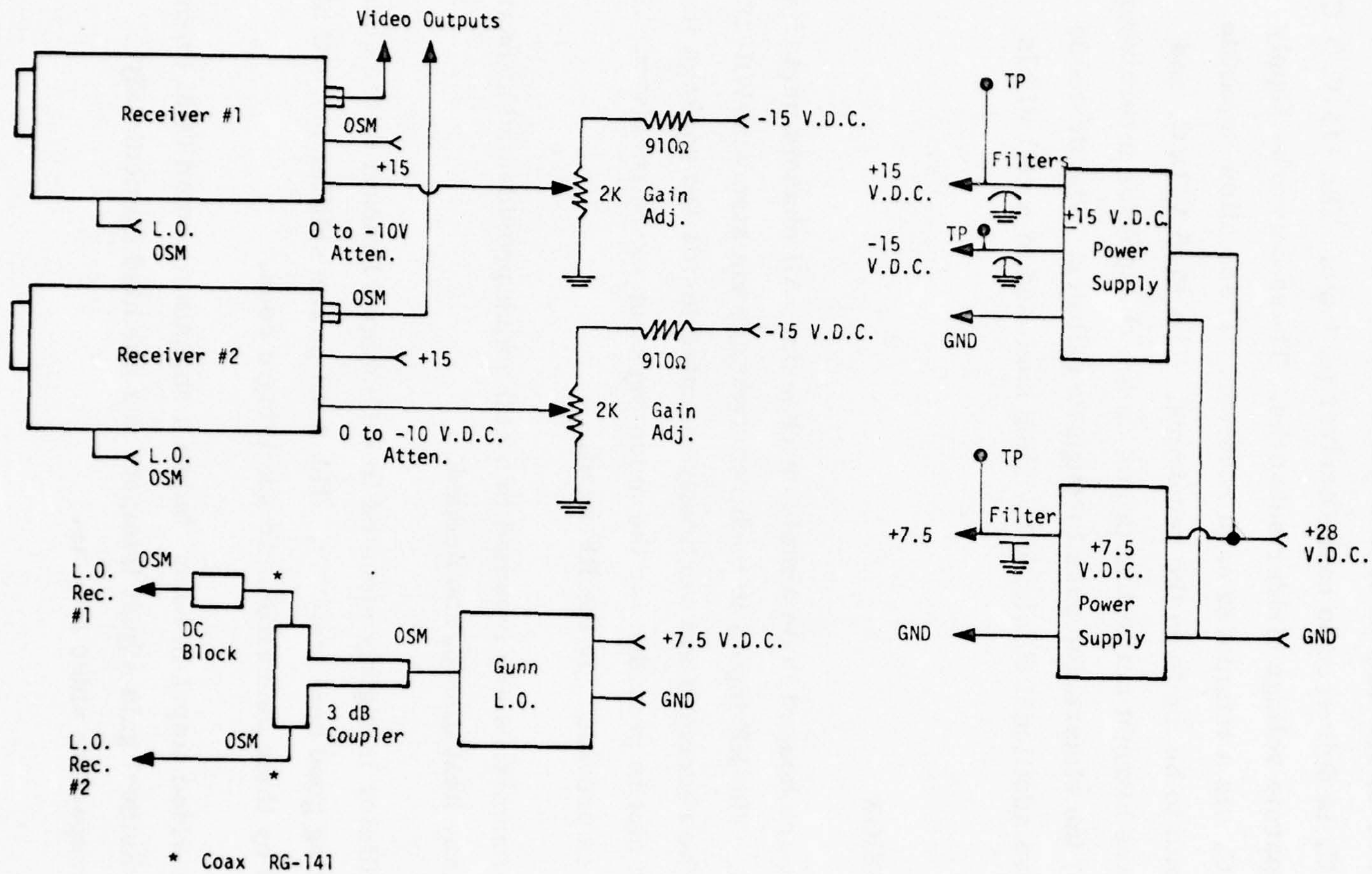

Figure 3-10. Multichannel Array Wiring

The +7.5 V.D.C. at 1.2 amp is used to power the Gunn effect local oscillator. The +15 V.D.C. is delivered to each receiver package. The -15 V.D.C. is wired to separate voltage divider networks. These networks supply 0 to -10 V.D.C. via a trimpot to each receiver. These allow separate gain adjustments to be made on the receivers. The +7.5 V.D.C. and $\pm$ 15 V.D.C. are brought out to test points on the chassis for monitoring. All voltages to the electronics pass through RFI filters. The dc-to-dc converters have additional shielding by being enclosed in a cell within the package.

PACKAGE DESIGN

The receivers are housed in an aluminum chassis. All chassis parts have been irridited. The RF inputs to each receiver are via standard WR-28 waveguide. The receivers are vertically mounted inside the package in a rack. A third slot is provided for the mounting of an extra receiver. A knockout plug is provided for the RF input.

The dc-to-dc converters are mounted in a cell which provides additional shielding and any heat dissipation needed.

The Gunn oscillator is rigidly mounted in a U-shaped bracket to the chassis bottom providing good heat transfer. The 3 dB power splitter and DC block are supported by their connections to semi-rigid coax.

Each receiver video output is connected to a chassis mounted OSM through coax. The individual gain adjust trimpots are mounted immediately behind their respective video outputs.

SECTION 4

PERFORMANCE TEST RESULTS

The data covered in this section responds directly to the test data items requested in the Work Statement of the contract. For each test data item evaluation procedures are described and test data presented.

The setups used in testing each receiver for various parameters are shown in Figures 4-1 and 4-2.

Figure 4-1 gives the basic noise figure test setup. In all noise figure tests, the detector is jumpered out with a wire and the IF appears on the output connector. The receiver is operated at minimum gain for these tests and a 20 dB pad is placed in the IF output so that the input to the Noise Figure Indicator (NFI) is within its dynamic range. The tunable signal generator provides a local oscillator input to the NFI for broadband measurements.

Figure 4-2 gives the test setup for measuring receiver gain, video transfer function, and RF dynamic range. The couplers were used to reduce the RF signal to a usable level.

RECEIVER NOISE FIGURE

Double-sideband noise figure data was taken on receiver No. 1 and No. 2 as functions of center frequency, IF bandwidth and local oscillator injection level. The basic noise figure measurement configuration is shown in Figure 4-1.

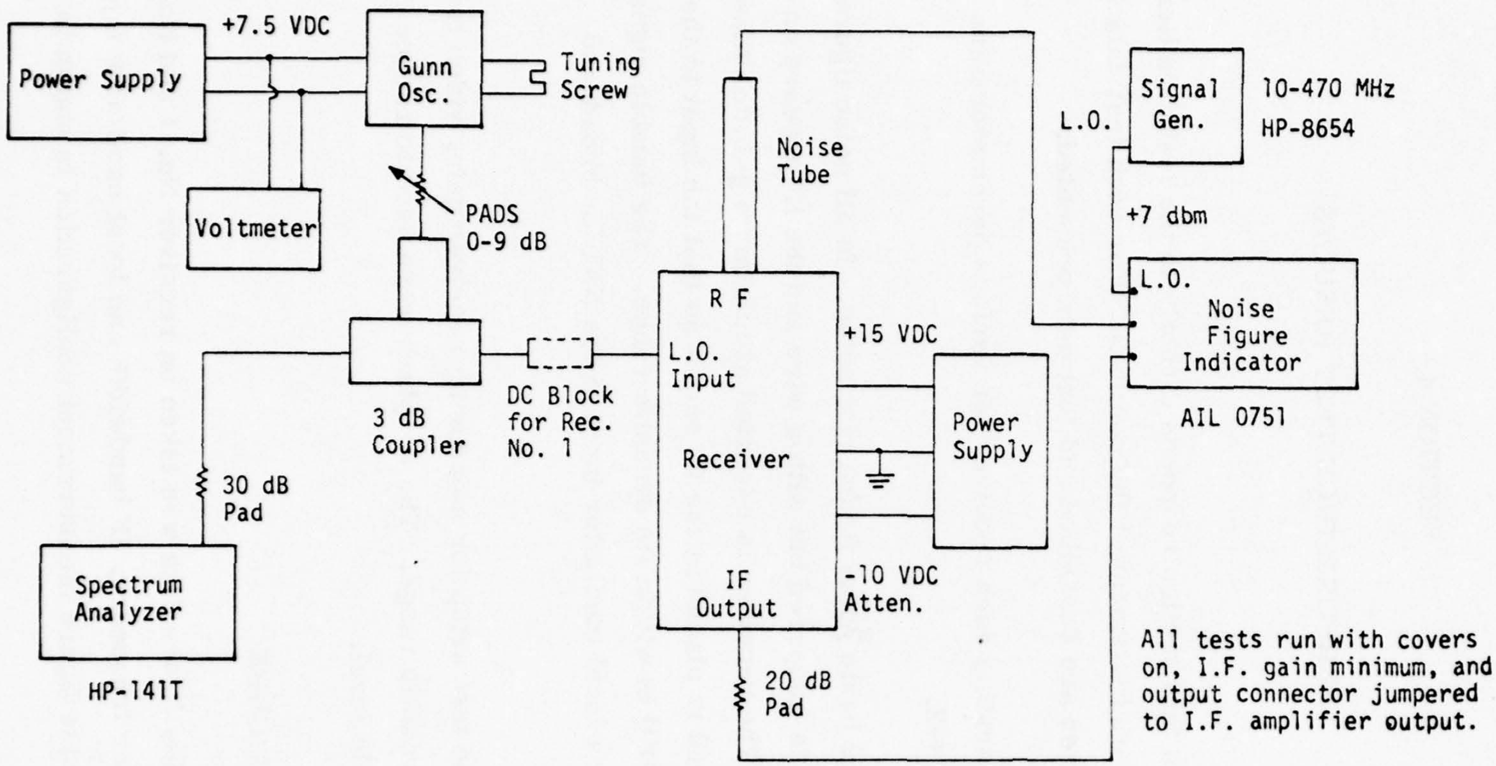

Figure 4-1. Noise Figure Test Setup

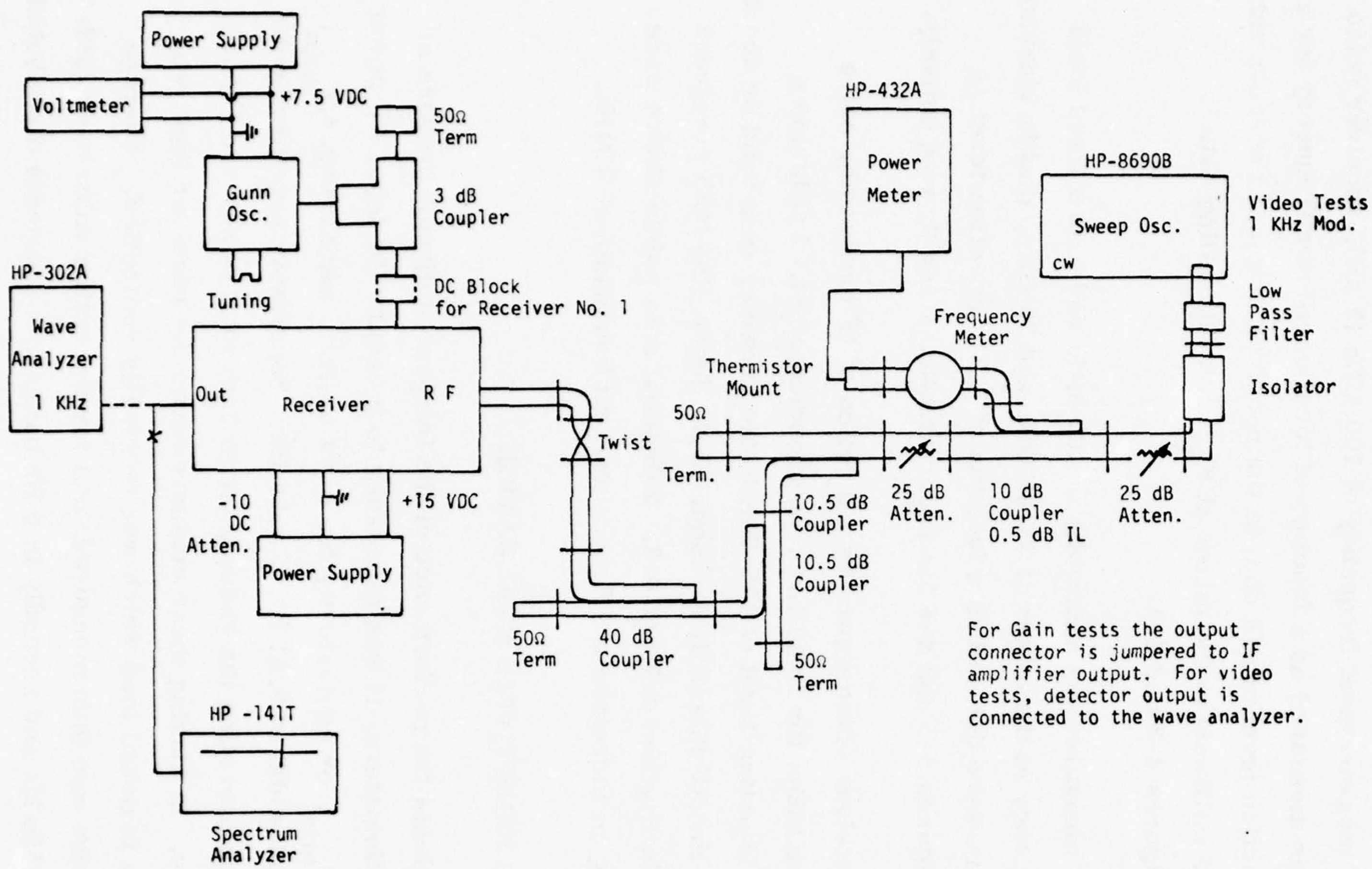

Figure 4-2. Gain Measurement Test Setup

With a fixed IF measurement frequency of 100 MHz (3 dB), receiver noise figure (dsb) was measured as a function of local oscillator frequency for a fixed L.O. injection level of +19 dbm to the receiver at x-band corresponding to roughly 5 milliwatt to the mixer at K_a band. Resulting data is presented in Figures 4-3 and 4-4.

With a fixed IF measurement bandwidth of 100 MHz and with a fixed local oscillator frequency at the mixer of 34.65 GHz and 35 GHz, double sideband noise figure data were derived as a function of L.O. injection level as presented in Figures 4-5 and 4-6 for receivers No. 1 and 2, respectively.

To establish receiver noise figure as a function of IF bandwidth, noise figure data were taken for fixed L.O. frequencies of 34.65 GHz and a constant L.O. injection level of +19 dbm to the receiver at x-band or about 5 milliwatts to the RF mixer at K_a band. Data describing both receivers are presented in Figures 4-7 and 4-8. Individual data points shown were measured using an incremental IF measurement bandwidth of 5 MHz.

RADIOMETRIC SENSITIVITY EVALUATION

In order to evaluate the performance of the integrated circuit sensors as total power radiometers, it was necessary to measure the input RF power sensitivity, ΔP_{min}, or equivalently the input thermal sensitivity, ΔT_{min}, over a video bandwidth of 0.01 Hz to 2500 Hz. Sensitivity measurements were made when operating the radiometer in both total power and Dicke switched modes. In making these measurements the receiver input was terminated in a matched load which was thermally controlled. Average video output noise was then measured first for the entire video bandwidth of 0.01 Hz to 2500 Hz and secondly in 6 Hz bandwidth segments distributed

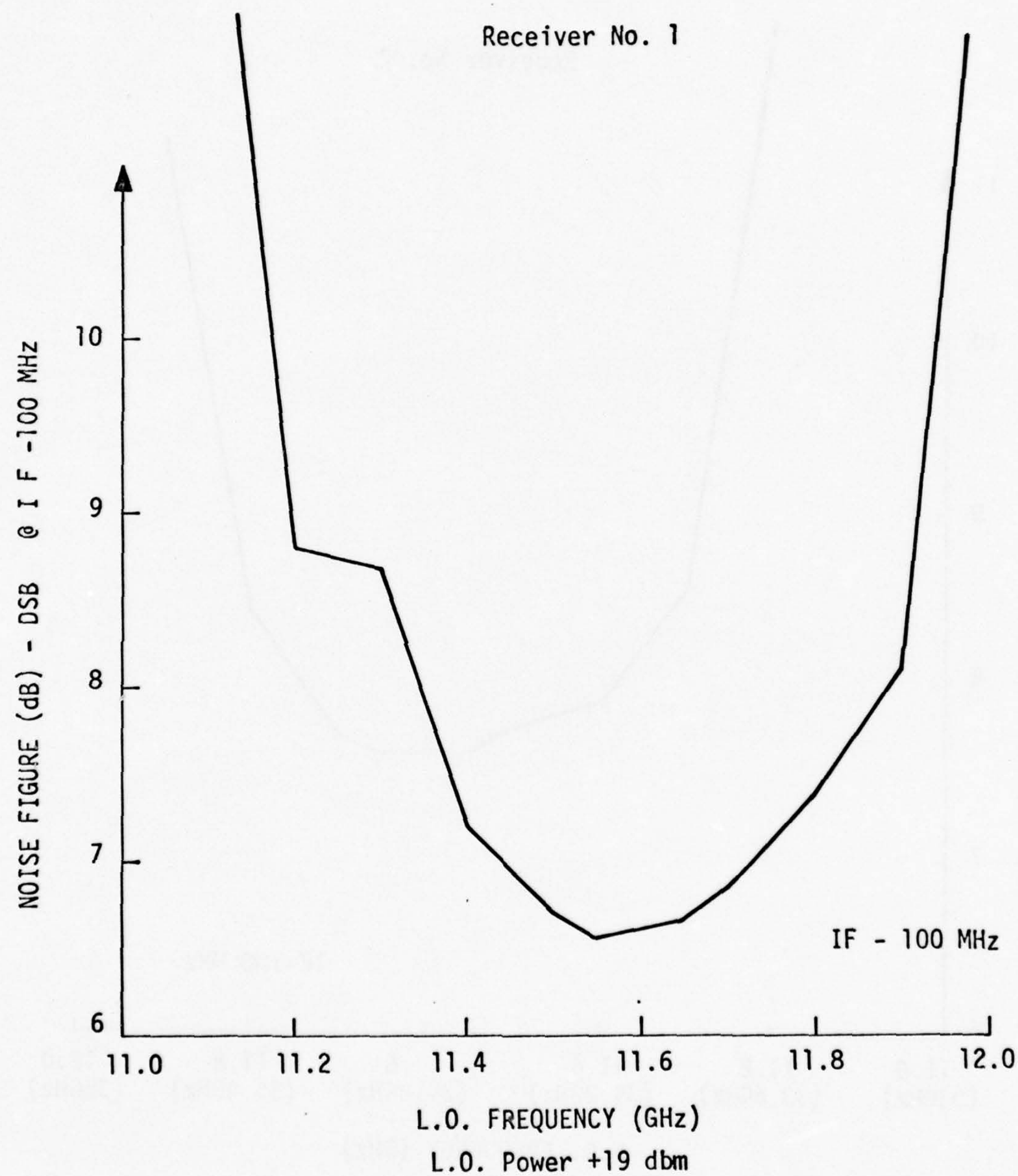

Figure 4-3. L.O. Frequency vs Noise Figure DSB

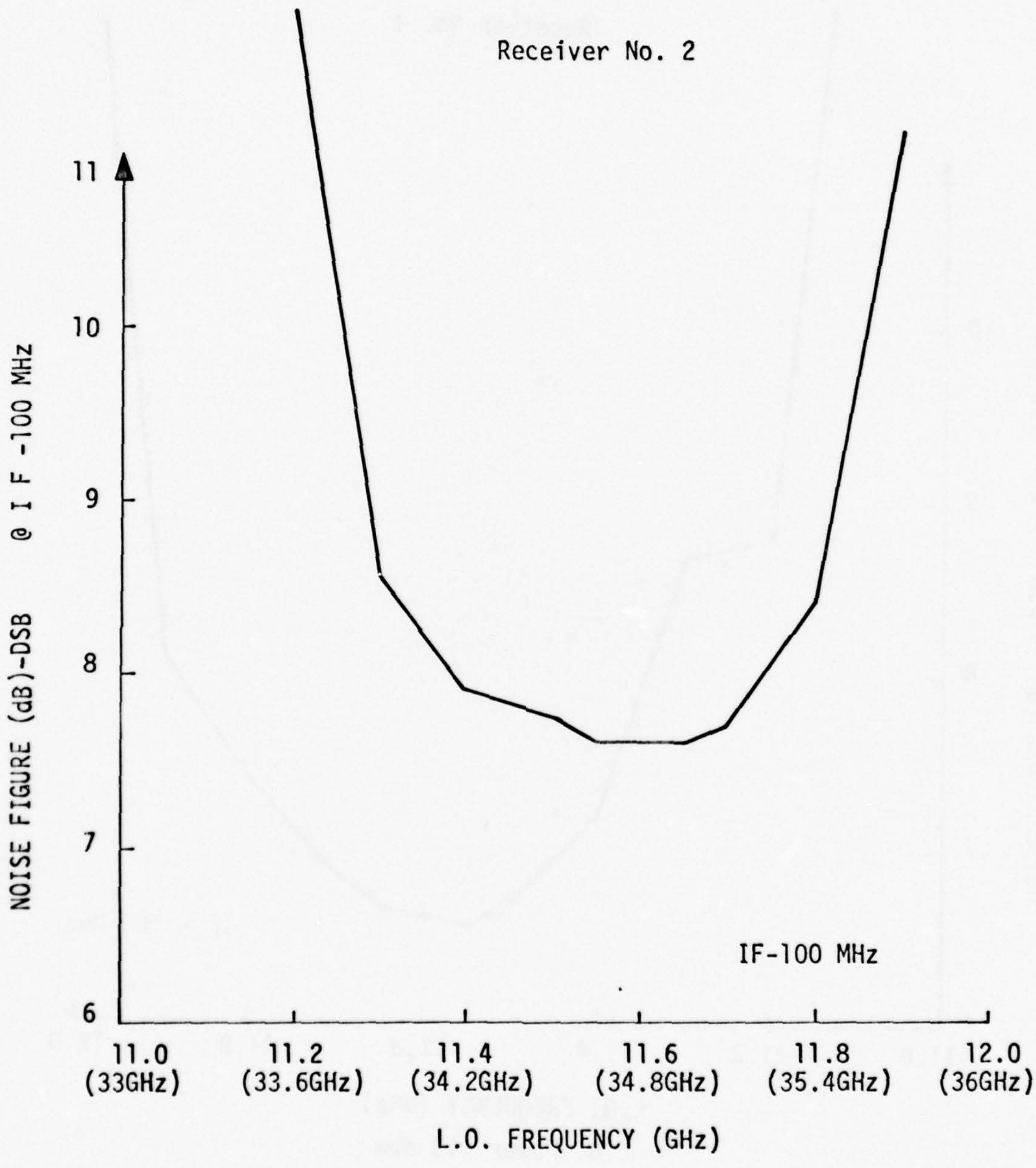

Figure 4-4. L.O. Frequency vs Noise Figure DSB

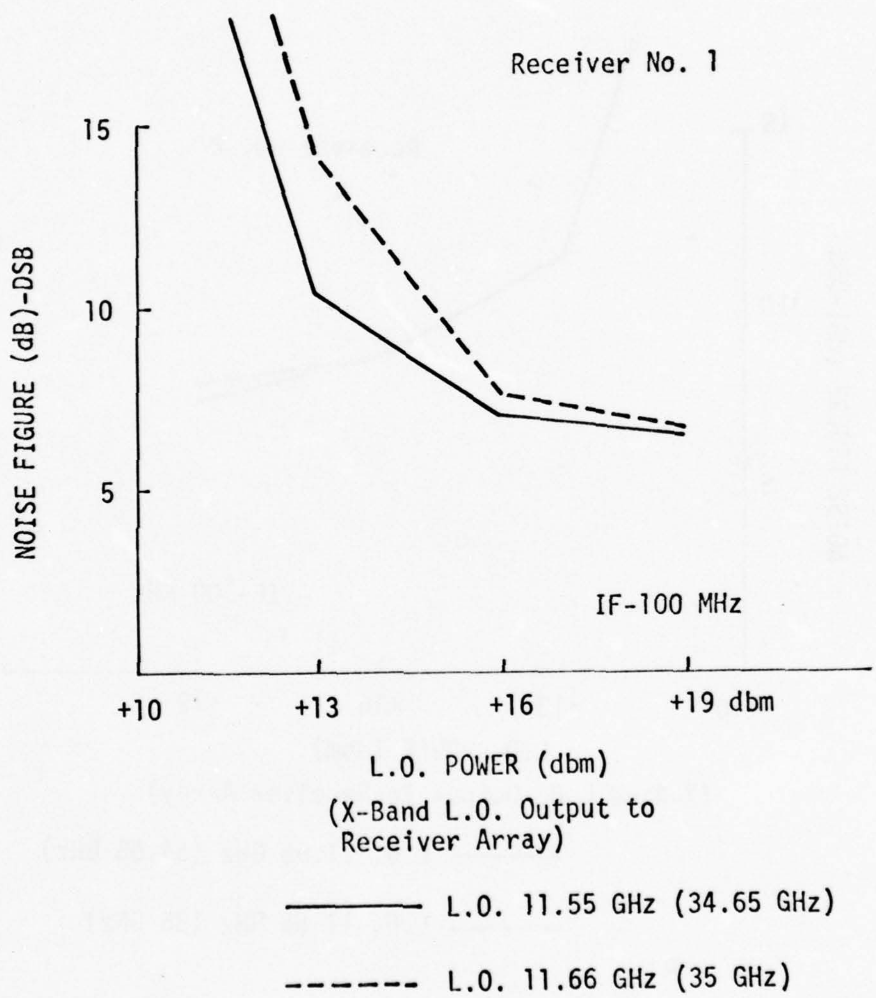

Figure 4-5. L.O. Power vs Noise Figure DSB

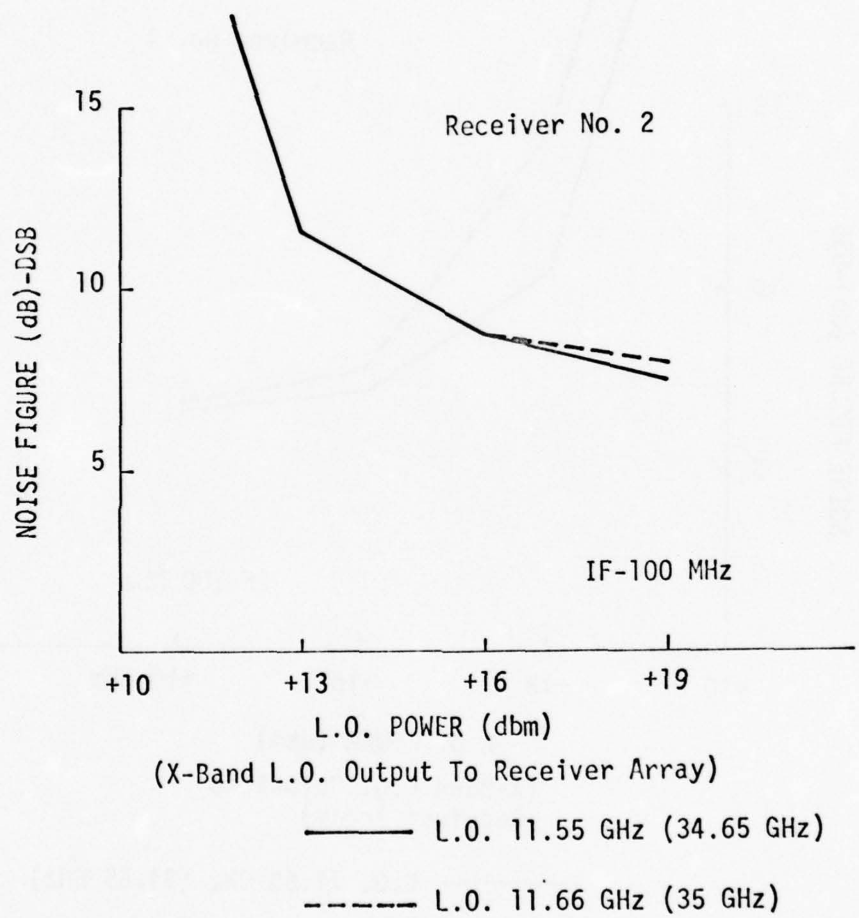

Figure 4-6. L.O. Power vs Noise Figure DSB

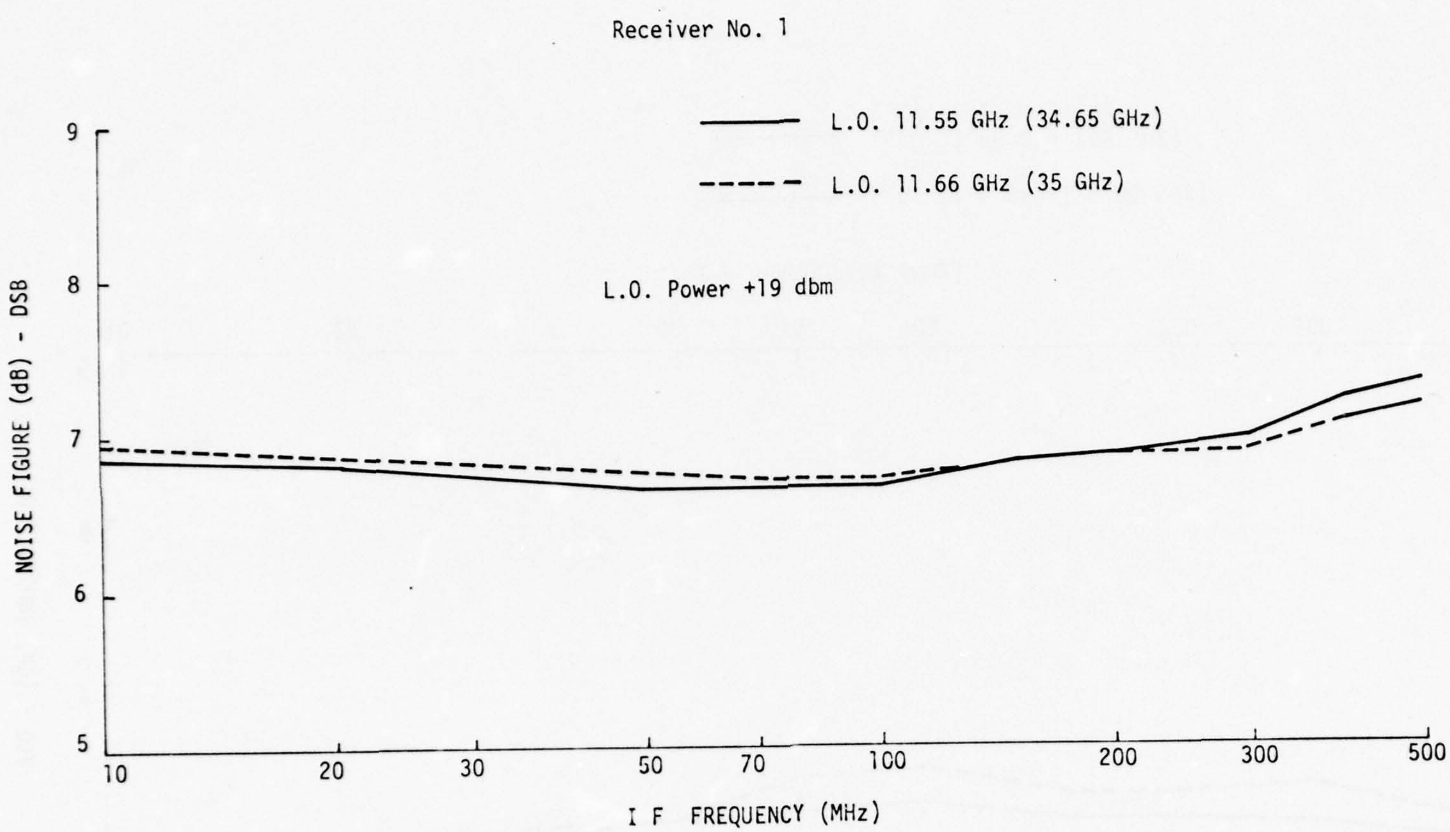

Figure 4-7. I F Frequency vs Noise Figure DSB

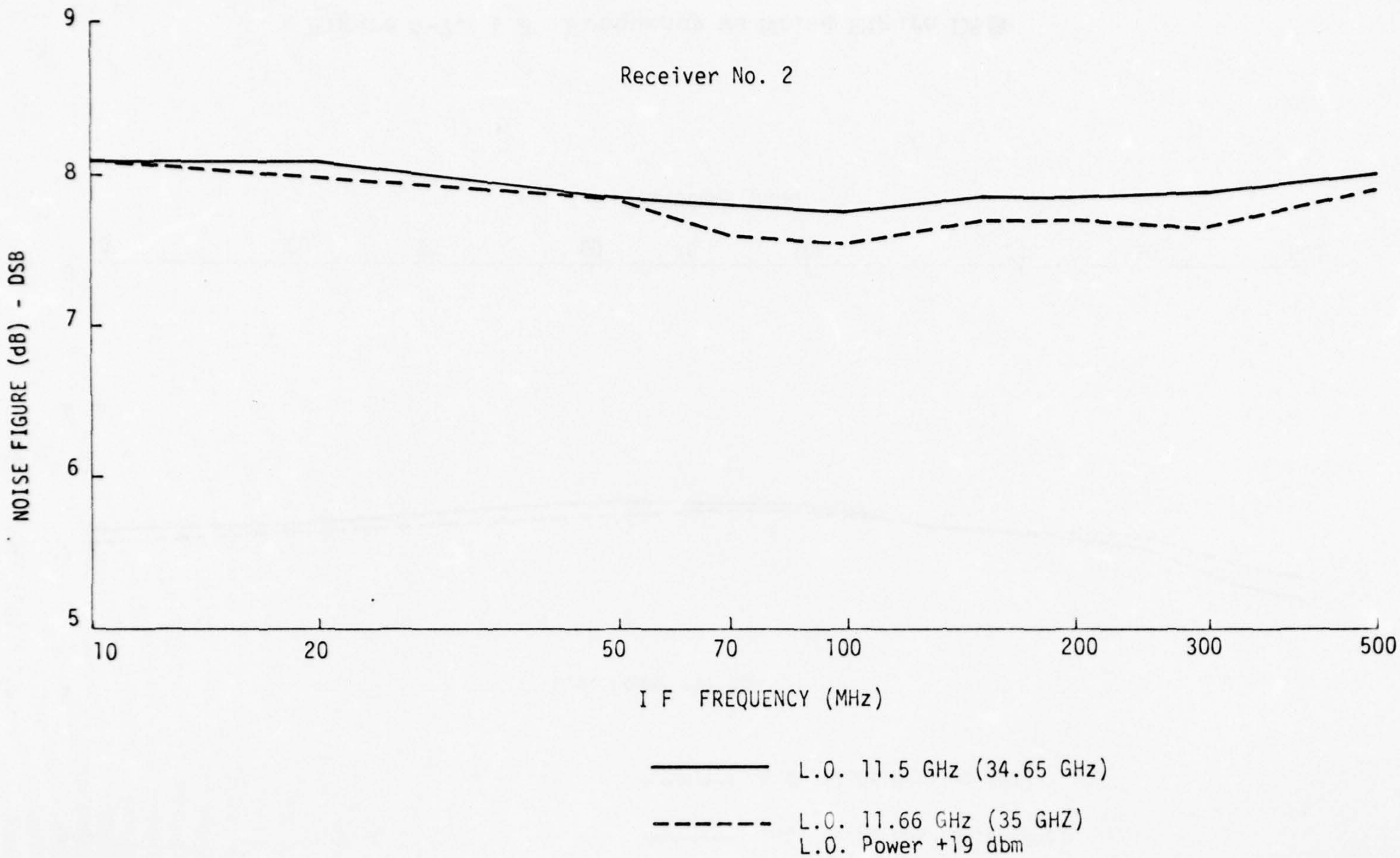

Figure 4-8. I F Frequency vs Noise Figure DSB

from 0.01 Hz to 2500 Hz. Experimental data indicate that, in the total power mode of operation, the I.C. sensor has a minimum detectable input power level of $\Delta P_{min} = 4.52 \times 10^{-14}$ watts. This corresponds to an input minimum detectable temperature of $\Delta T_{min} = 2.34°K$ assuming an operating RF bandwidth of 1.4 GHz. In the Dicke switched mode, the minimum detectable input power and temperatures were 1×10^{-13} watts and 5.5°K, respectively.

The experimental configuration for the total power mode tests is illustrated in Figure 4-9. With this test configuration the rms receiver noise was measured in two steps for bandwidths of 0.01 Hz to 10 Hz and for 10 Hz to 2500 Hz. In each case calibration of the measurement circuit was accomplished by replacing the receiver with a 50 ohm matched termination. Results of these measurements are indicated below.

Bandwidth Range	Calibration Noise Voltage (rms)	Test Noise Voltage (rms)	Receiver Equivalent Noise Voltage (rms)	ΔP_{min} (Watts)	ΔT_{min} (1.4 GHz B.W.) (°K)
0.01 to 10 Hz	.0003 V	.0012 V	$1. \times 10^{-5}$ V	2.5×10^{-15}	0.13°K
10 to 2500 Hz	.0030 V	.0210 V	1.8×10^{-4} V	4.52×10^{-14}	2.34°K

Thus the thermal sensitivity of the receiver over the total video bandwidth of 0.01 Hz to 2500 Hz is approximately $\Delta T_{min} = 2.5°K$ (rms). For a receiver integration time of one second, this corresponds to a minimum detectable temperature of less than one-tenth degree Kelvin.

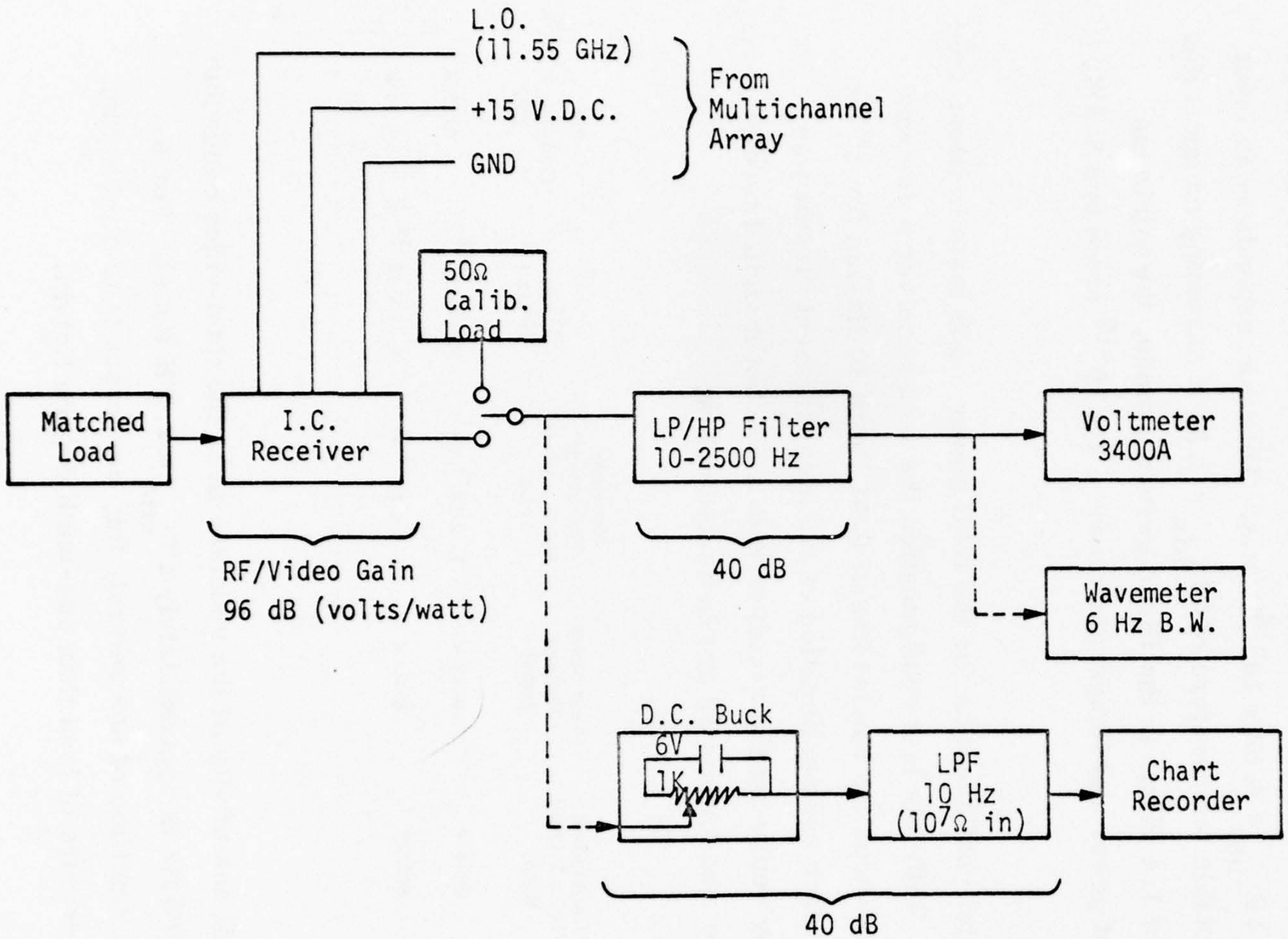

Figure 4-9. Total Power Radiometer Test Configuration

Additional noise measurements were made for total power operating mode utilizing the H. P. wave analyzer to establish noise voltage levels in GHz bandwidths at selected frequencies over the range of 10 to 2500 Hz. The wave analyzer voltage readings are presented in Figure 4-10.

The receiver sensitivity was next measured when operating in the Dicke switched mode. The test configuration is illustrated in Figure 4-11. The rms receiver noise was again determined over frequency increments of 0.01 Hz to 10 Hz and 10 Hz to 2500 Hz using the chart recorder and rms voltmeter, respectively. The resulting data is presented below.

Bandwidth Range	Calibration Noise Voltage (rms)	Test Noise Voltage (rms)	Receiver Equivalent Noise Voltage (rms)	ΔP_{min} (Watts)	ΔT_{min} (1.4 GHz B.W.) (°K)
0.01 - 10 Hz	0.001 V	0.123 V	1.23×10^{-5} V	3×10^{-15} W	0.15°K
10 - 2500 Hz	0.700 V	5.000 V	4.3×10^{-4} V	1×10^{-13} W	5.50°K

In these tests the two input matched loads were thermally stabilized at 298°K prior to Dicke mode receiver testing. There was no convenient way to calibrate the phase angle receiver in these measurements. The calibration noise level shown in the data above was derived when a 50 ohm matched termination was used to replace the PAR at the input of the band-pass filter.

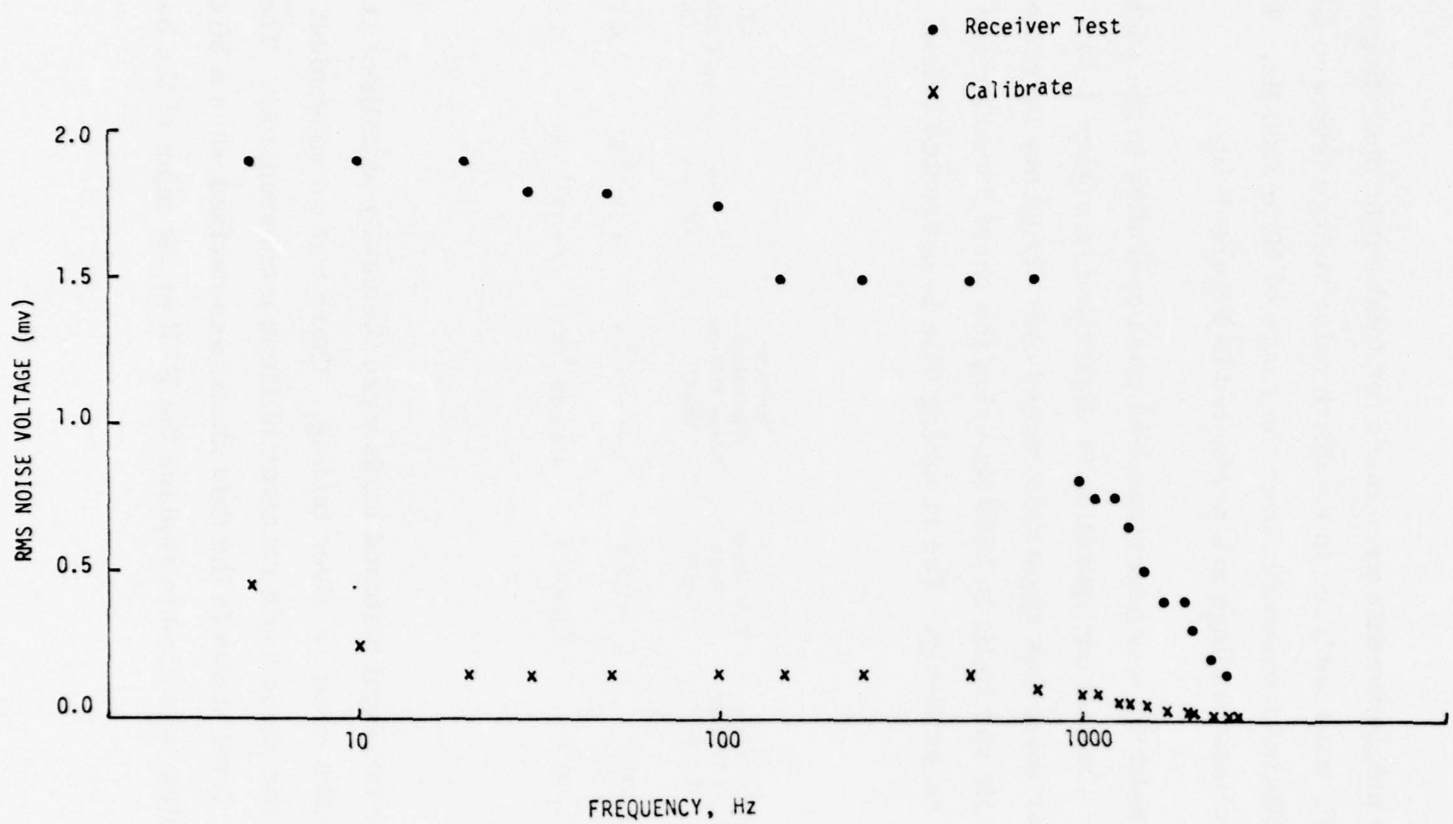

Figure 4-10. Total Power Radiometer RMS Noise Voltage at H. P. Wavemeter (6 Hz Bandwidth)

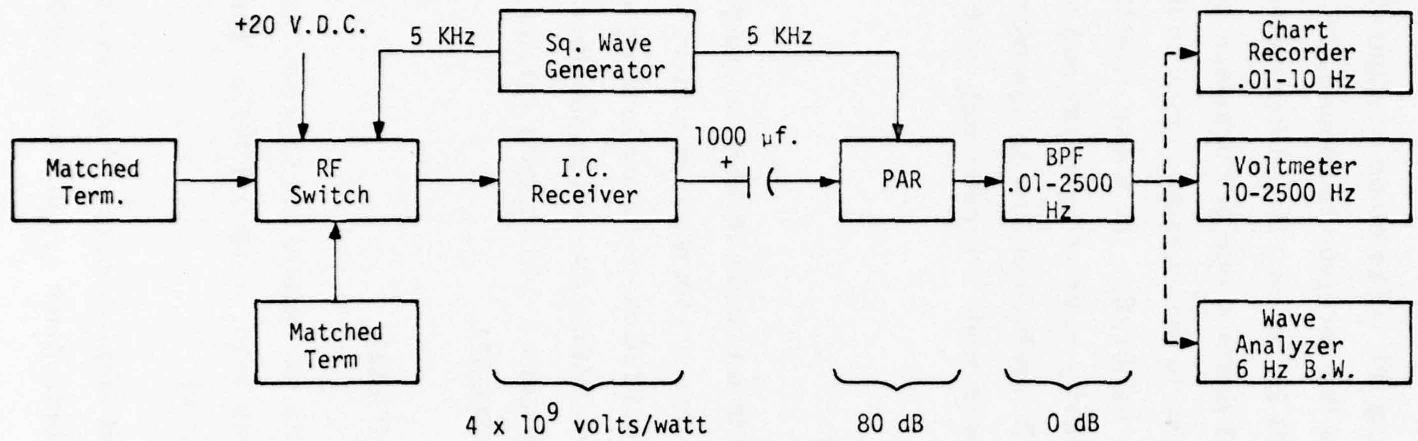

Figure 4-11. Dicke Switched Radiometer Test Configuration

The test data indicate that, using the Dicke mode configuration, the minimum detectable noise temperature of the receiver is about 5.6°K when measured over the video bandwidth of 0.01 Hz to 2500 Hz. Unexpectedly, this is slightly degraded from the total power mode performance measured previously. This is probably due to inaccuracies made in the Dicke measurement arising from not properly calibrating the phase detection loop. One would expect Dicke mode sensitivity to be at least as good or better than the total power performance. It can be concluded, however, that the I.C. receivers operating in total power mode are extremely stable over the video operating bandwidth.

IF GAIN VERSUS FREQUENCY

The IF gains were measured with a tunable leveled signal generator, and the amplifier outputs were monitored with a power meter. Figures 4-12 and 4-13 give data on the two SDP-8278 packages used in the receivers. The data also show the slight gain variations due to temperature cycling (between -30°C and 55°C) of each unit. Figure 4-14 is a gain versus frequency plot of a typical preamplifier UTO-511.

IF GAIN VERSUS SUPPLY VOLTAGE

The data measured on the IF gain variations due to power supply voltage changes are presented in Figures 4-15, 4-16 and 4-17. The same test setup as mentioned above was used.

The data taken on three different amplifiers are shown on each graph as the power supply voltage is varied. Each graph shows a different frequency (50, 300, 550 MHz).

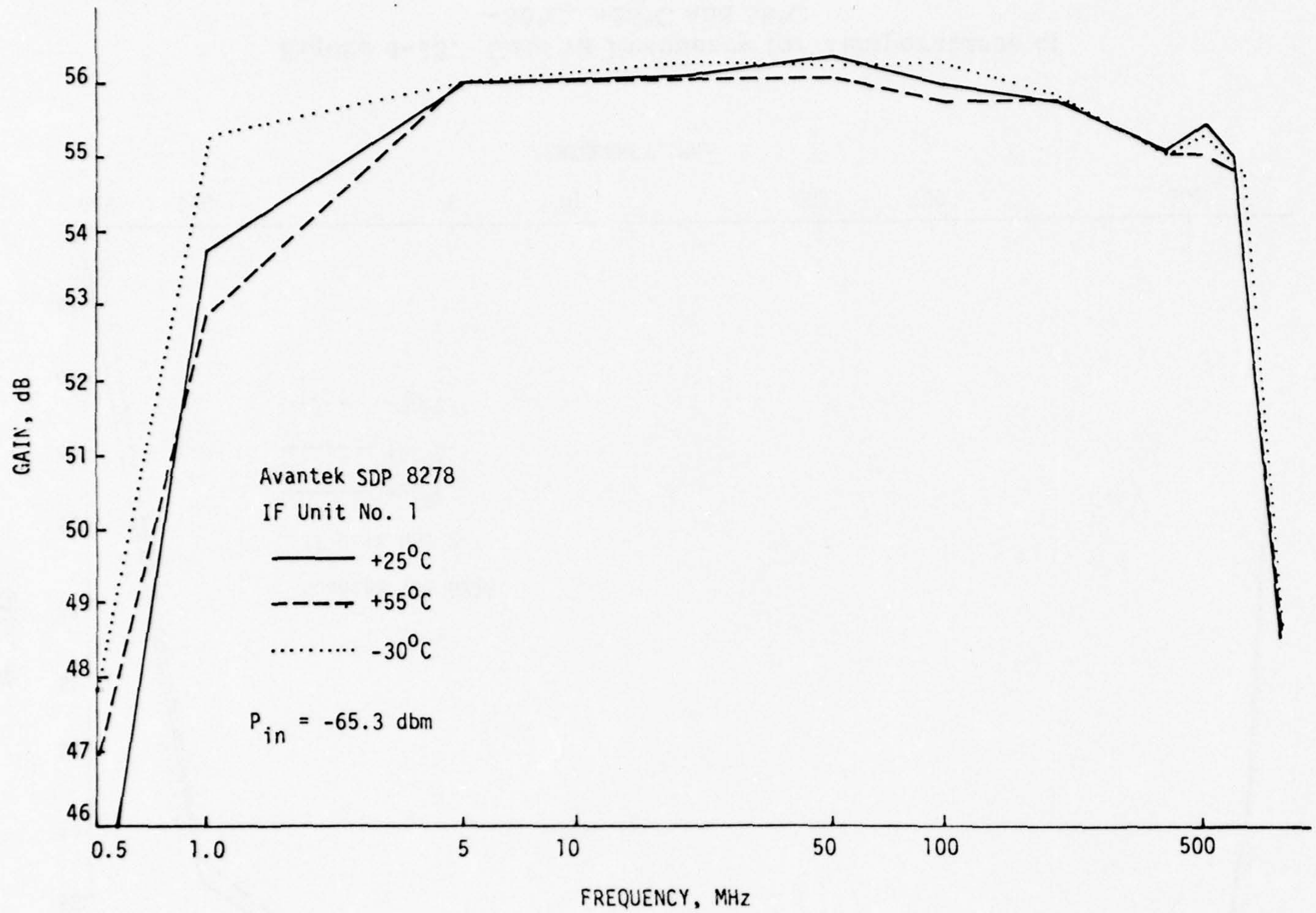

Figure 4-12. Gain vs Frequency for Temperatures of -30°C, +25°C and +55°C

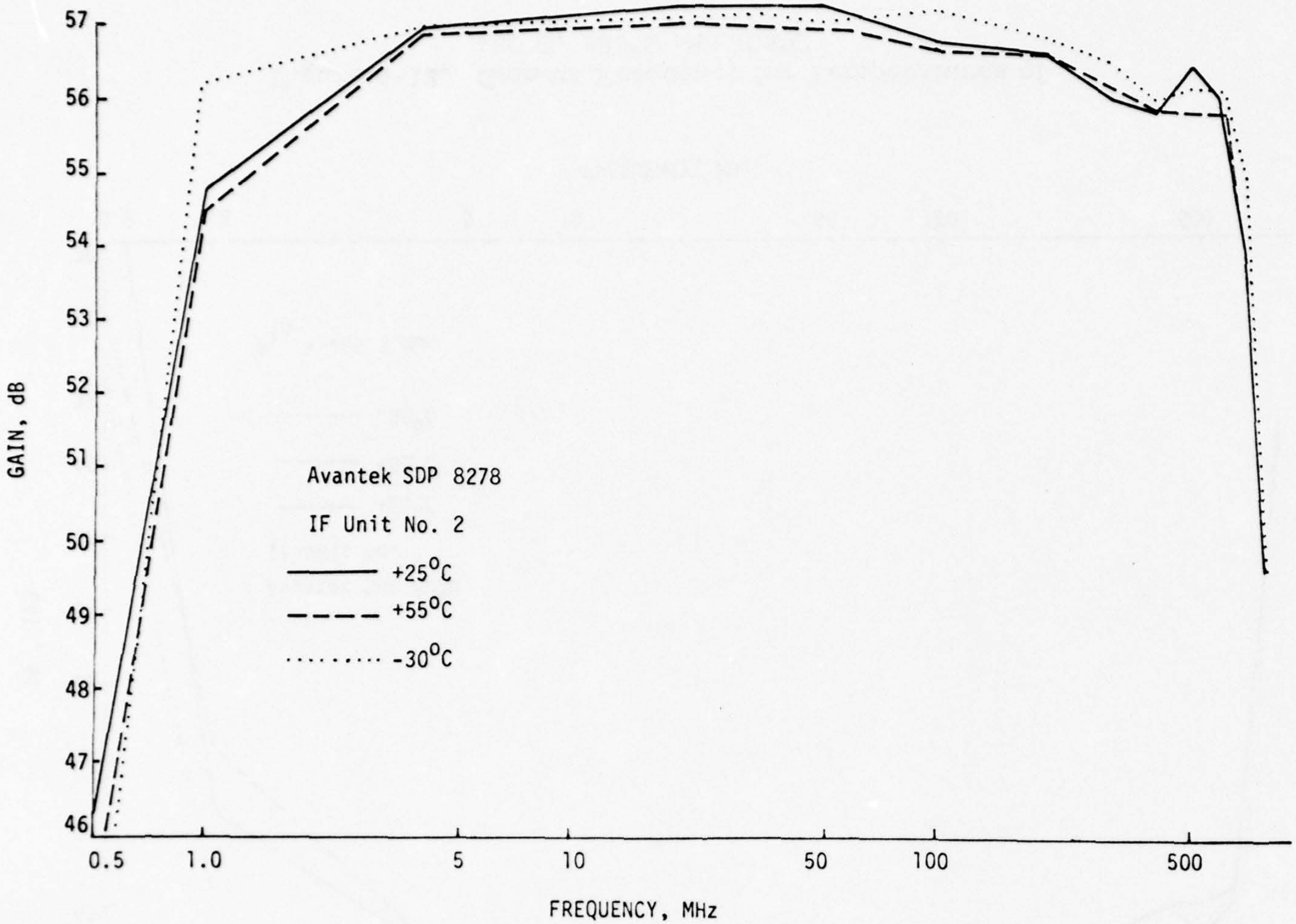

Figure 4-13. Gain vs Frequency for Temperatures of -30°C, +25°C and 55°C

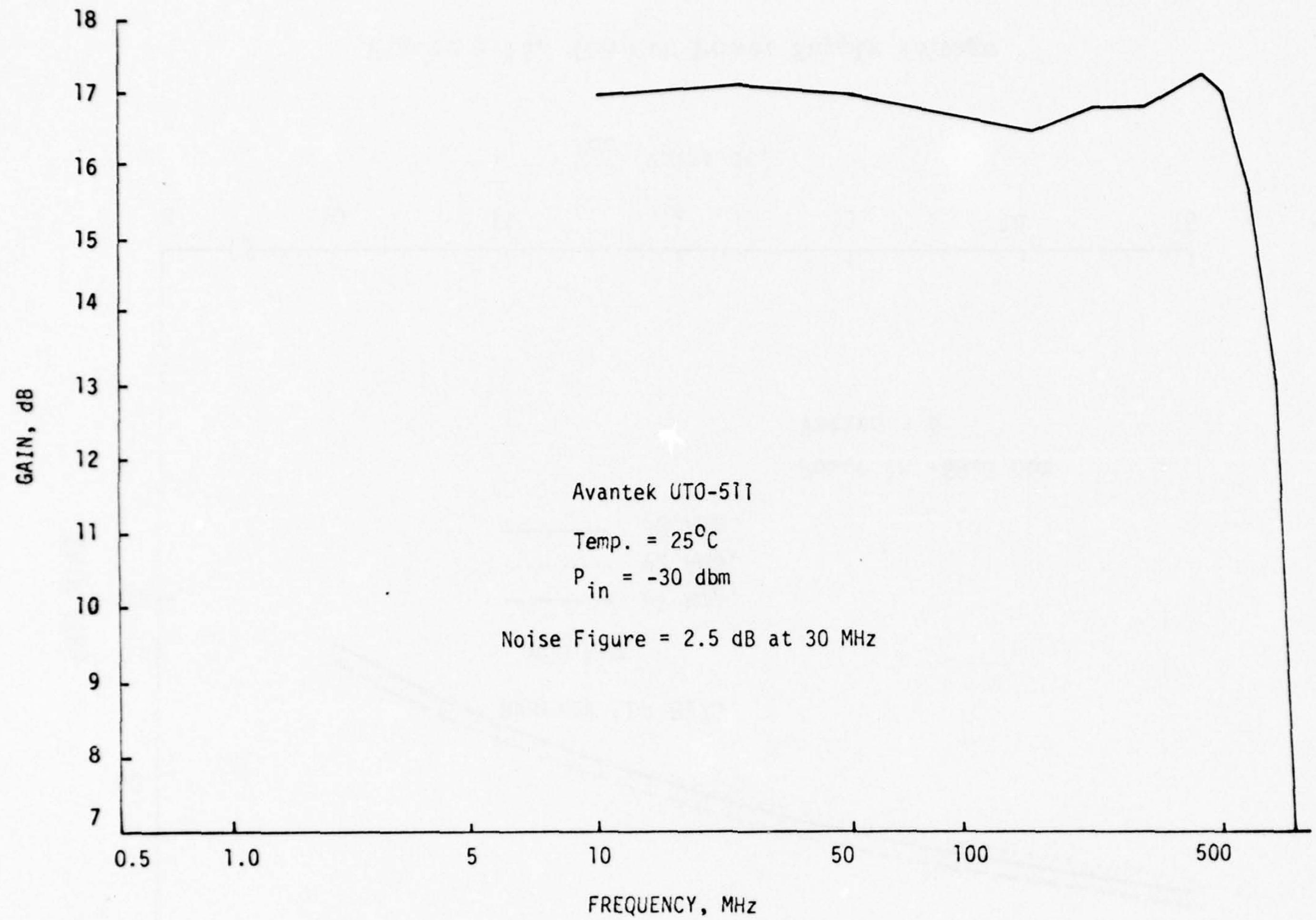

Figure 4-14. Gain vs Frequency of Avantek Pre-Amp

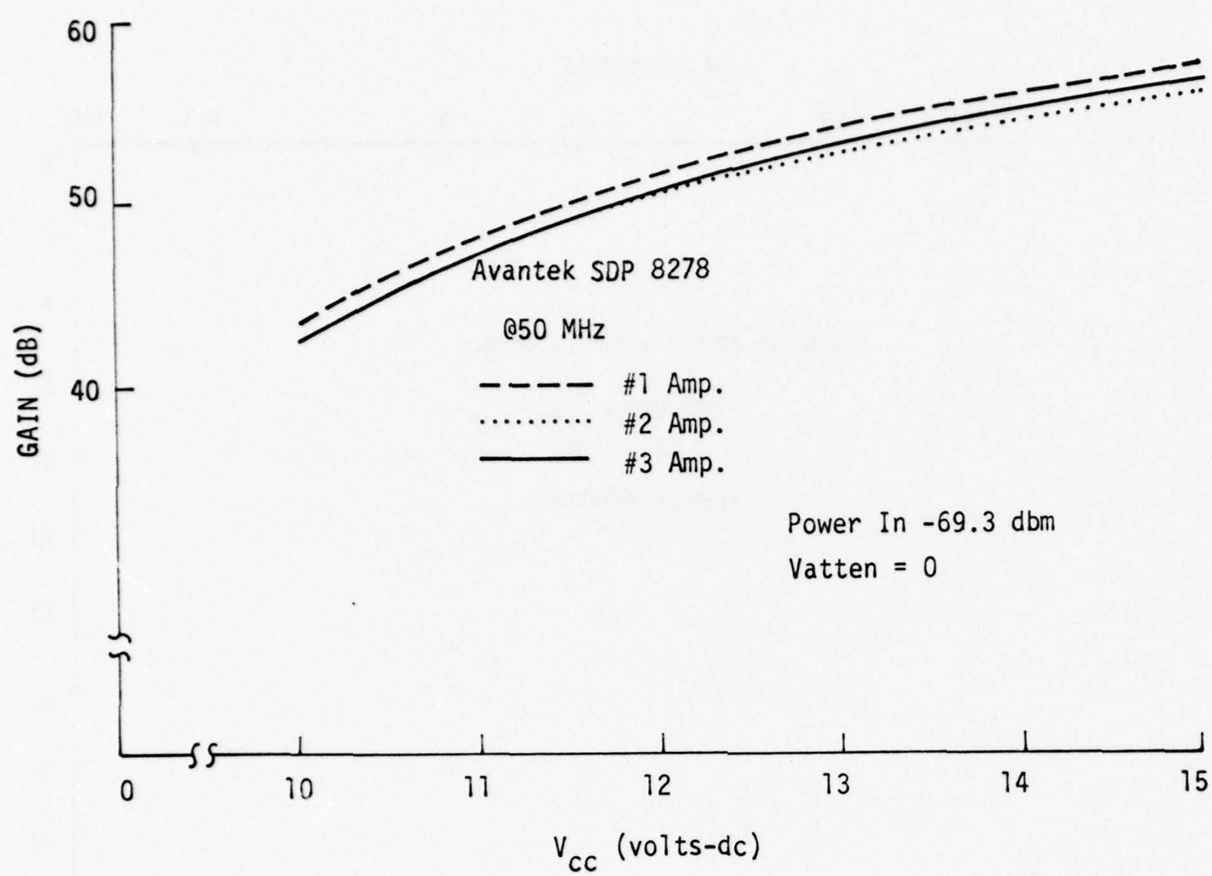

Figure 4-15. Gain vs Power Supply Voltage

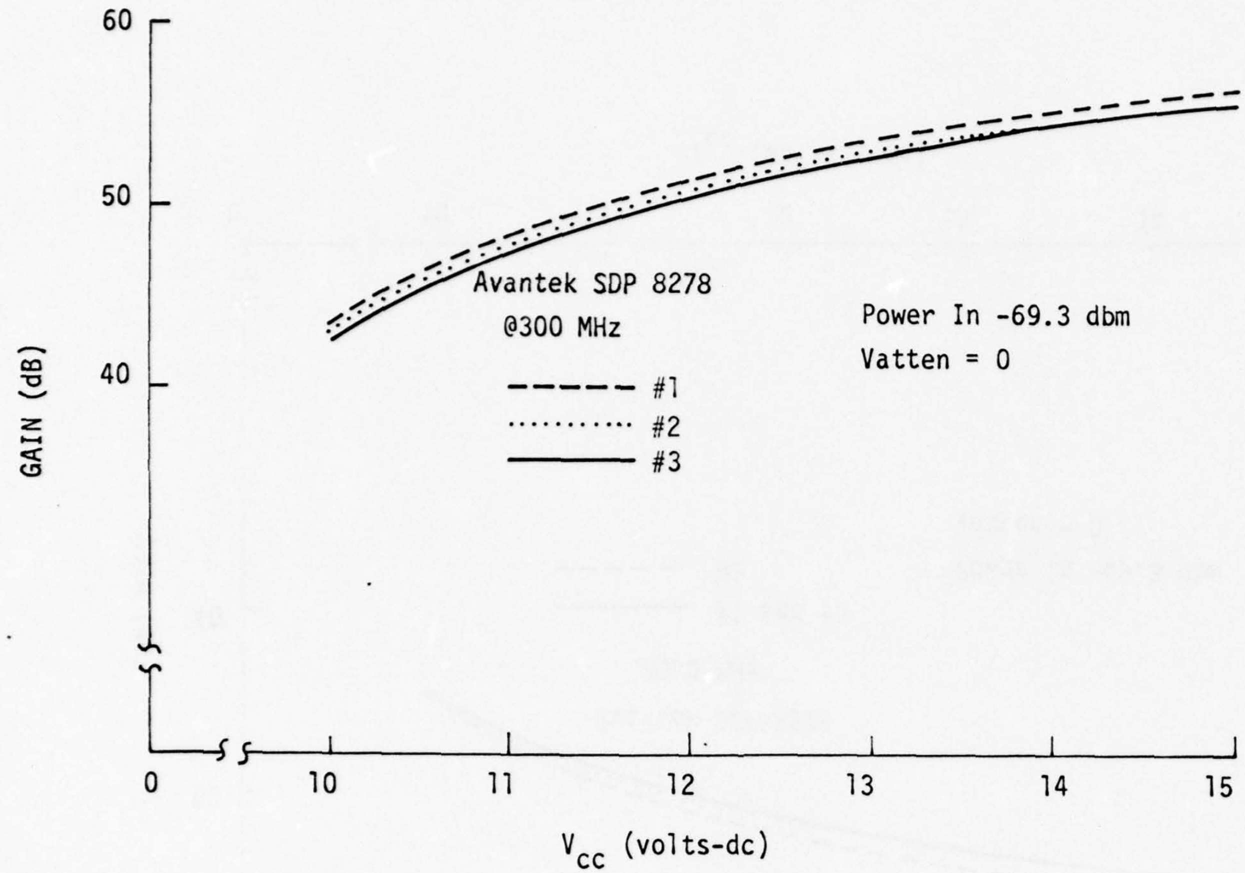

Figure 4-16. Gain vs Power Supply Voltage

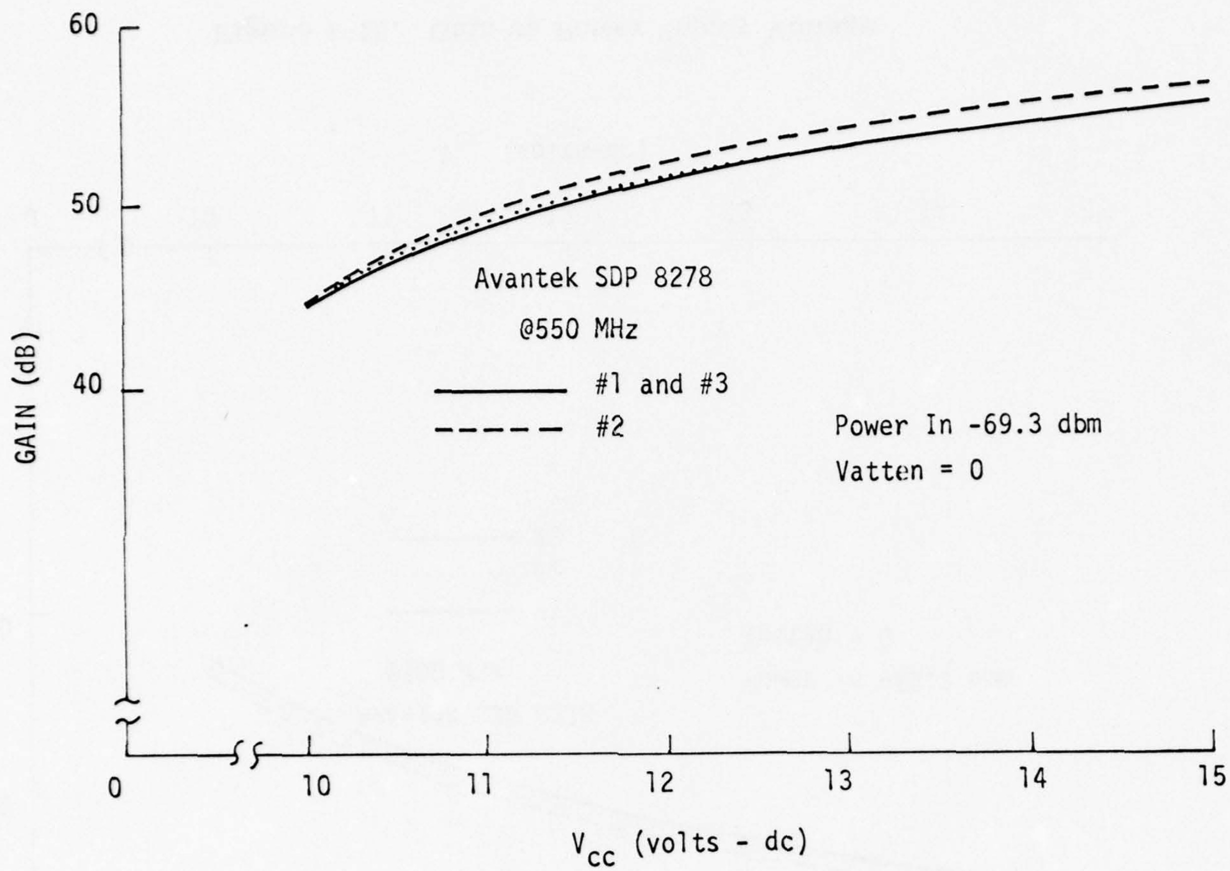

Figure 4-17. Gain vs Power Supply Voltage

RF/VIDEO TRANSFER GAIN VERSUS TEMPERATURE

The setup in Figure 4-2 was used to measure the RF to video transfer function. The receiver was placed in the temperature chamber and a thermistor placed on the case. The receiver was operated at maximum gain and the output monitored with the wave analyzer. The RF signal was connected to the receiver via waveguide through a port in the chamber. The L.O. power, video, and all power leads are also brought out through this port.

The data taken are presented in Figure 4-18. The initial data taken at room temperature (case temperature: 32°C) were normalized and appear as the straight base line. The receiver was then slowly lowered to -30°C and the deviation plotted. The receiver was next slowly brought to +55°C and the deviation again plotted. After these measurements were taken, the receiver was allowed to come back to room temperature and final data were taken.

The total deviations encountered in the video output line were about 1.5 mvrms during the temperature cycling.

RF BANDWIDTH

The RF bandwidth was determined by measuring the RF-to-video transfer function using the test setup of Figure 4-2. The RF power level was kept constant, and a 1 kHz modulation used. The receiver gain was at maximum and the detector was monitored with the wave analyzer.

The results are presented in Figures 4-19 and 4-20.

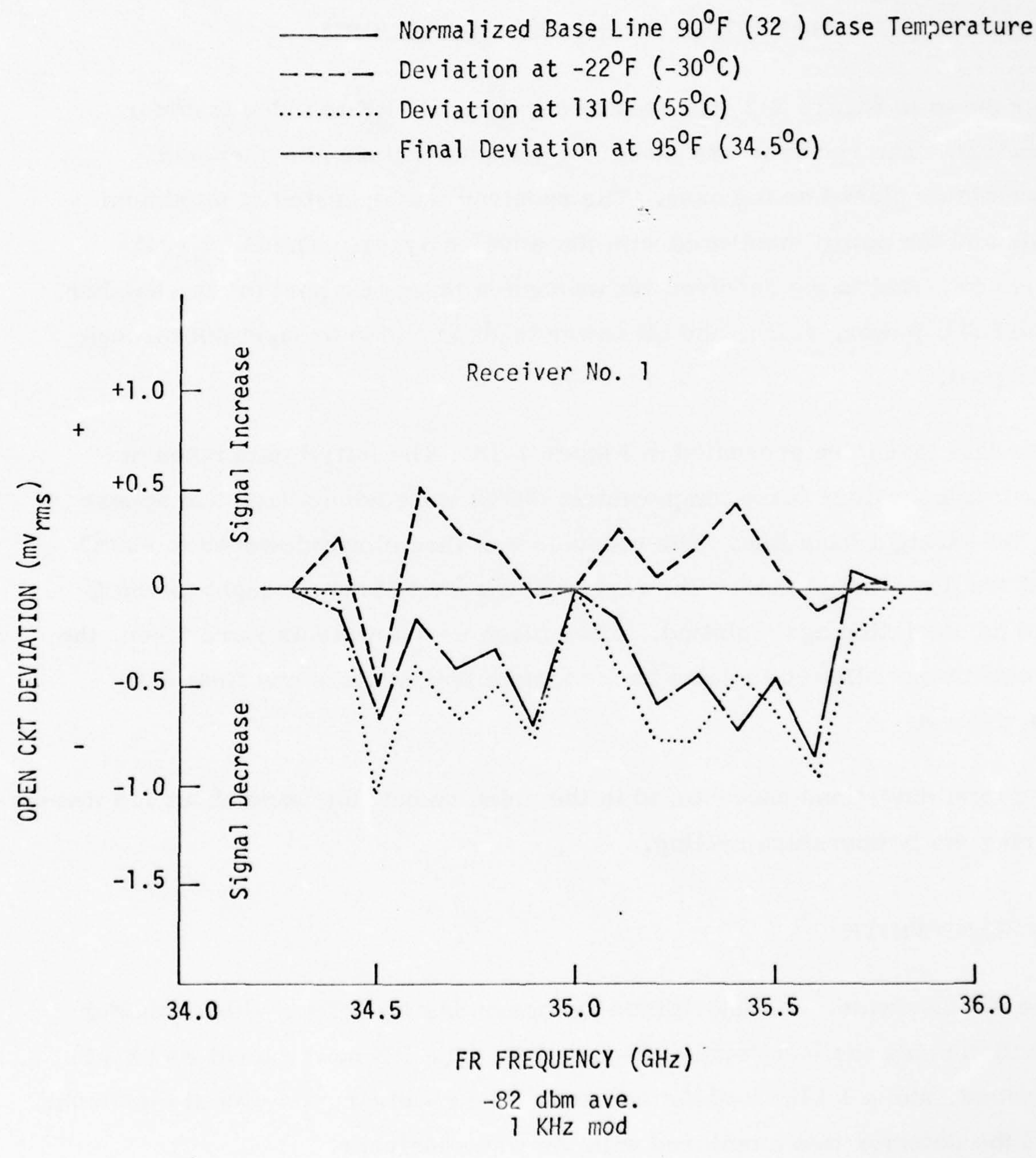

Figure 4-18. Temperature Chamber Receiver Tests

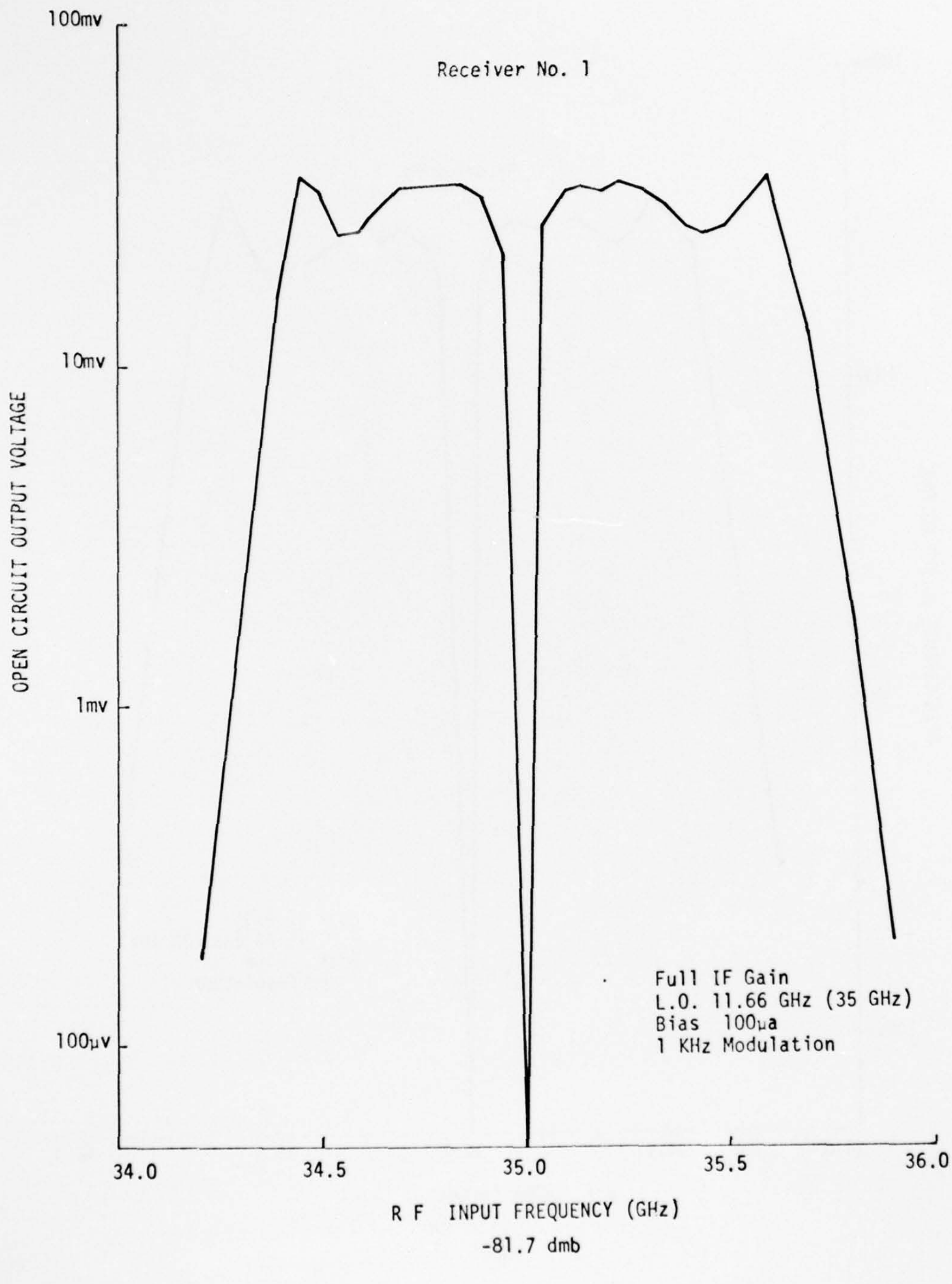

Figure 4-19. Video Output Voltage vs RF Input Frequency

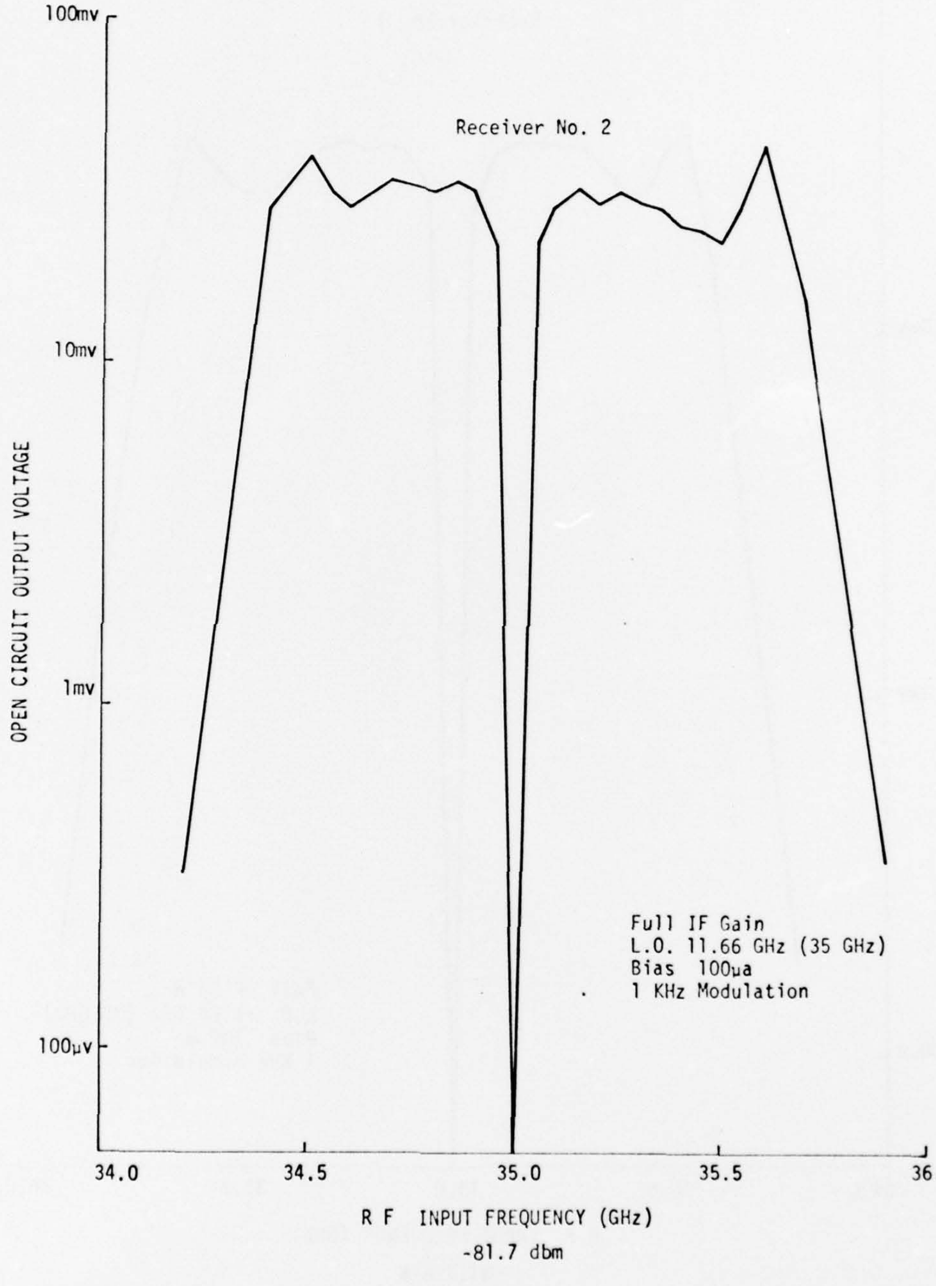

Figure 4-20. Video Output Voltage vs RF Input Frequency

RECEIVER DYNAMIC RANGE

The receiver dynamic range was measured using the test setup of Figure 4-2. The RF signal had a 1 kHz modulation and was operated at 100 MHz above the local oscillator-mixer frequency. (35.1 GHz) The RF power level was varied using variable attenuators and fixed pads. The detector output was monitored using the wave analyzer tuned to 1 kHz. The receivers were operated at maximum IF gain.

These data taken on each receiver are presented in Figures 4-21 and 4-22.

MULTIPLIER EFFICIENCY

A direct measurement of the efficiency of the multipliers in the receiver modules was not possible. Instead, efficiency was measured indirectly using the mixers themselves as indicators of L.O. output power at 35 GHz. From earlier individual measurements of the mixers, it was known that the mixer conversion loss reaches a minimum value as a function of increasing L.O. power at an L.O. injection level of about 5.6 milliwatts. From Figure 4-5 which illustrates receiver noise figure as a function of X-band L.O. input power, it can be seen that a corresponding minimum or flattening in receiver noise figure occurs for an X-band L.O. input level of about 100 milliwatts. Using these data the multiplier efficiency was roughly estimated to be about 5 to 6 percent. This is compared to a theoretical maximum efficiency of about 11 percent for this Schottky multiplier. A theoretical maximum of about 33 percent is estimated for a snap-varactor multiplier; however, the problem of impedance matching and mounting low cost diodes is difficult.

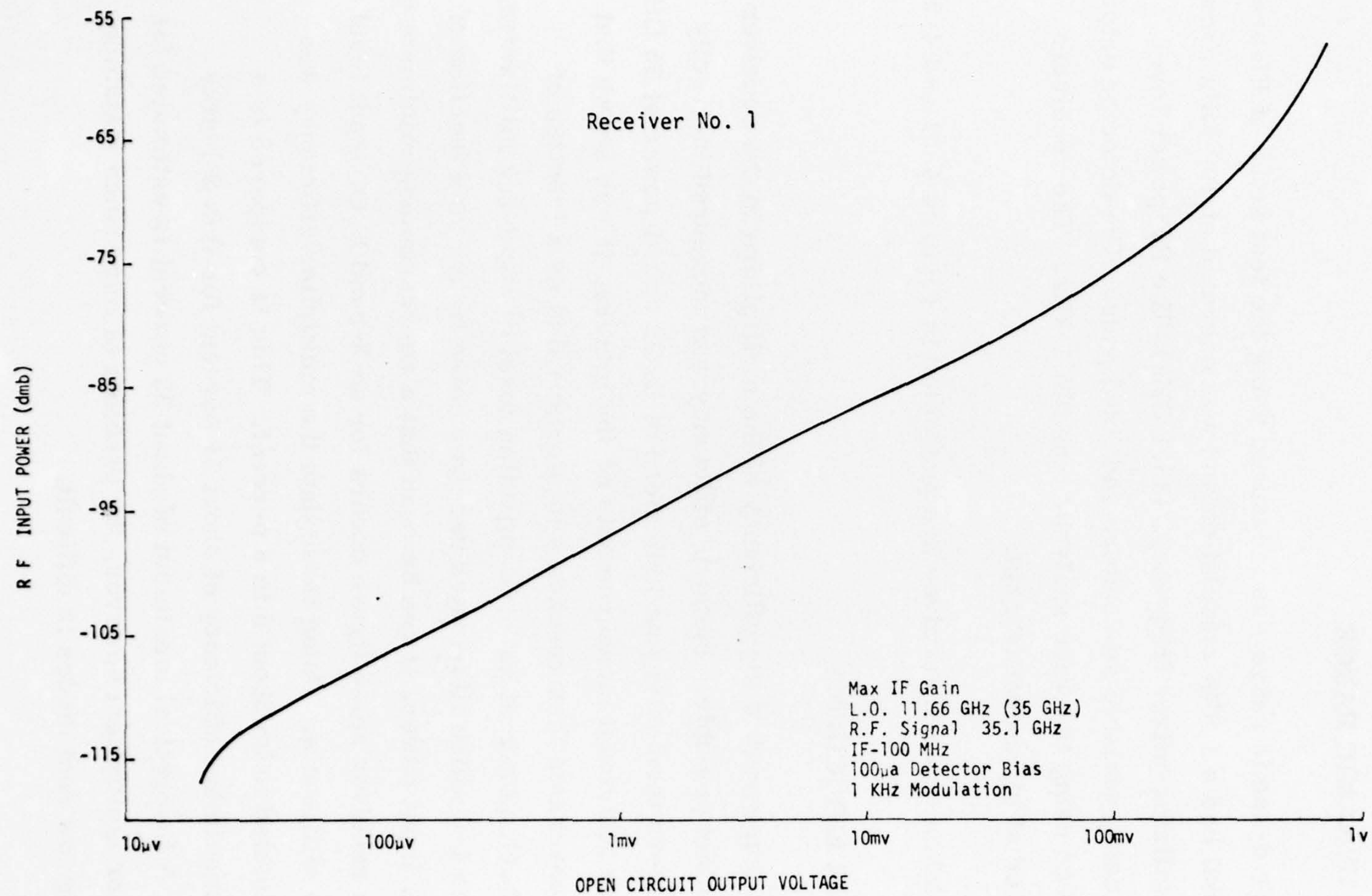

Figure 4-21. Video Output Voltage vs RF Input Power

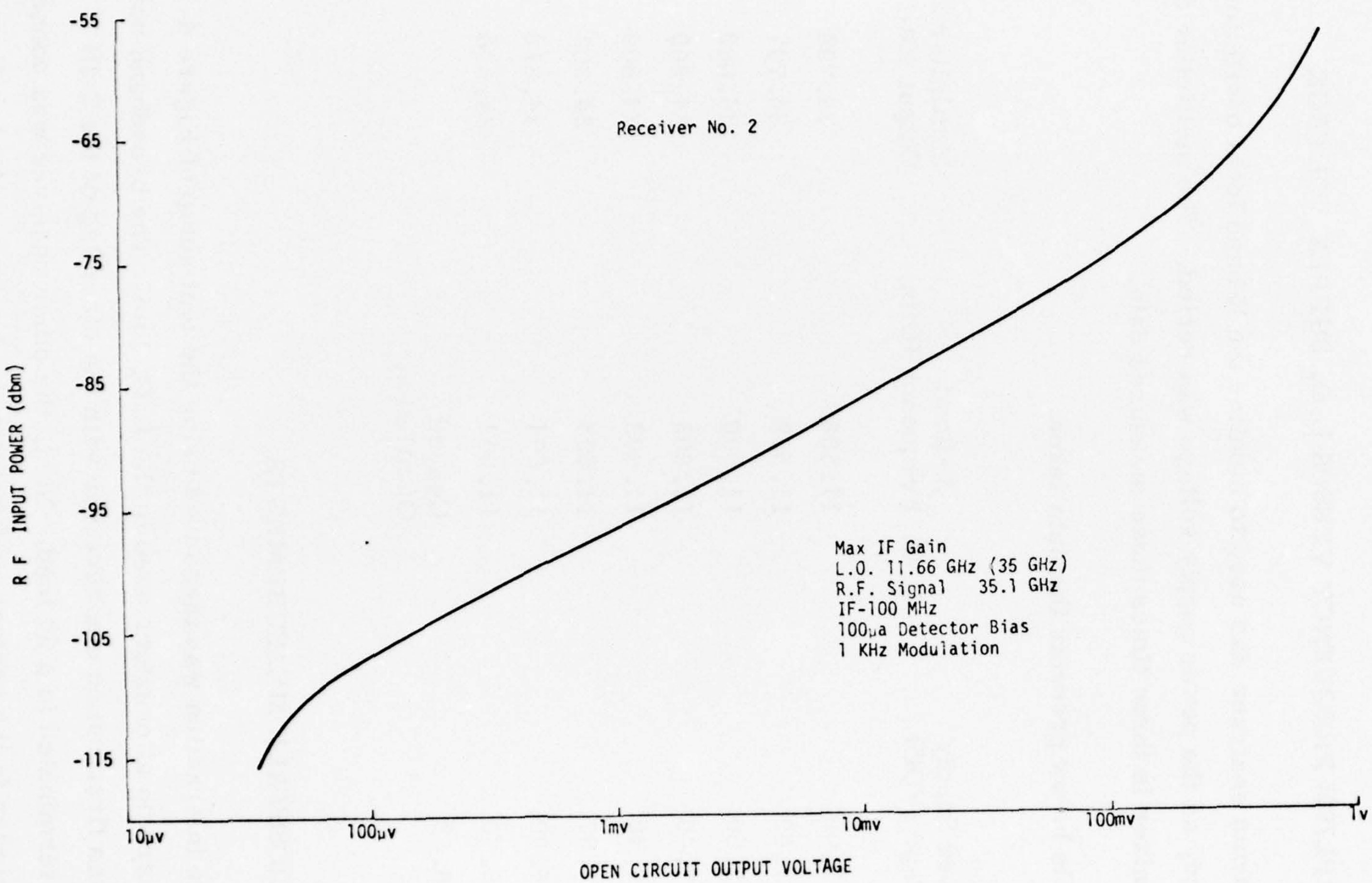

Figure 4-22. Video Output Voltage vs RF Input Power

MULTIPLIER FREQUENCY VERSUS L.O. SUPPLY VOLTAGE

A spectrum analyzer was used to monitor the X-band local oscillator frequency as the power supply voltage was varied. The multiplier output to the mixer is three times these measured data.

The table below presents the data taken.

Power Supply Voltage (VDC)	X-Band L.O. Frequency (GHz)	Multiplier x3 Output (GHz)
7.00	11.598	34.794
7.60	11.599	34.797
7.50	11.600	34.800
7.40	11.603	34.809
7.10	11.603	34.809
7.00	11.603	34.809
6.90	11.604	34.812
6.70	11.602	34.606
6.52	Ceased Oscillation	-

L.O. CROSSTALK MEASUREMENTS

Receiver interaction was measured using the test setup of Figure 4-1. There were no attenuators used in the L.O. line. The broadband noise figure was first run on one receiver with the other leg of the 3 dB coupler terminated in a 50 load. Next, the other receiver was connected to the coupler in the normal configuration and power applied. No

termination was placed on the RF input port of the second receiver. The broadband noise figure was again run.

Figure 4-23 and 4-24 present the data taken on this test. The noise figure on receiver No. 1 is basically unchanged, while on receiver No. 2 a slight improvement is seen. This is probably due to VSWR effects on the L.O. line.

PLANAR ANTENNA EVALUATION

Radiation pattern data and order of magnitude efficiency data have been compiled for a 35 GHz planar antenna which is currently being developed by Honeywell under internal investment funding. These data are being presented in this final report since this type of flat or conformal antenna may have future application in conjunction with I.C. radiometers of the type developed in this contract.

The planar antenna under test was Model No. RA-2 and consisted of a parallel plate disc resonator which was center-fed and loaded with a spiral slot. The parallel plate spacing of 0.060 inches was maintained using a teflon-loaded fiberglass dielectric, $\epsilon_r = 2.45$. The resonator was 7 inches in diameter and electrically shorted along its outside circumference. A spiral slot was etched in the top surface conductor of the disc resonator beginning at a radius of 1 inch and spiralling outward at a rate of 0.22 inches per turn for a total of nine complete turns. The slot width varied linearly from 0.020 inches at the center to 0.005 inches at the outside. The operating center frequency of the antenna was nominally 35.4 GHz.

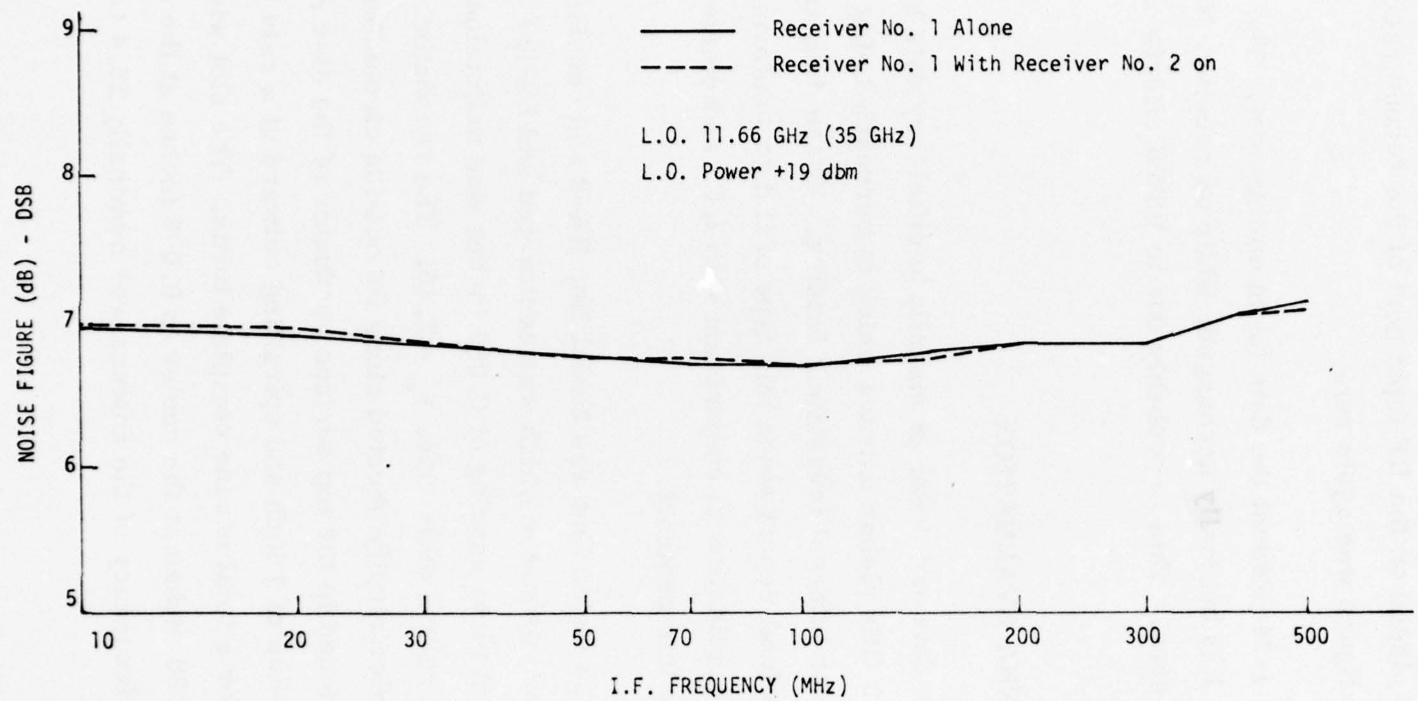

Figure 4-23. Receiver Interaction on Noise Figure
Receiver No. 1

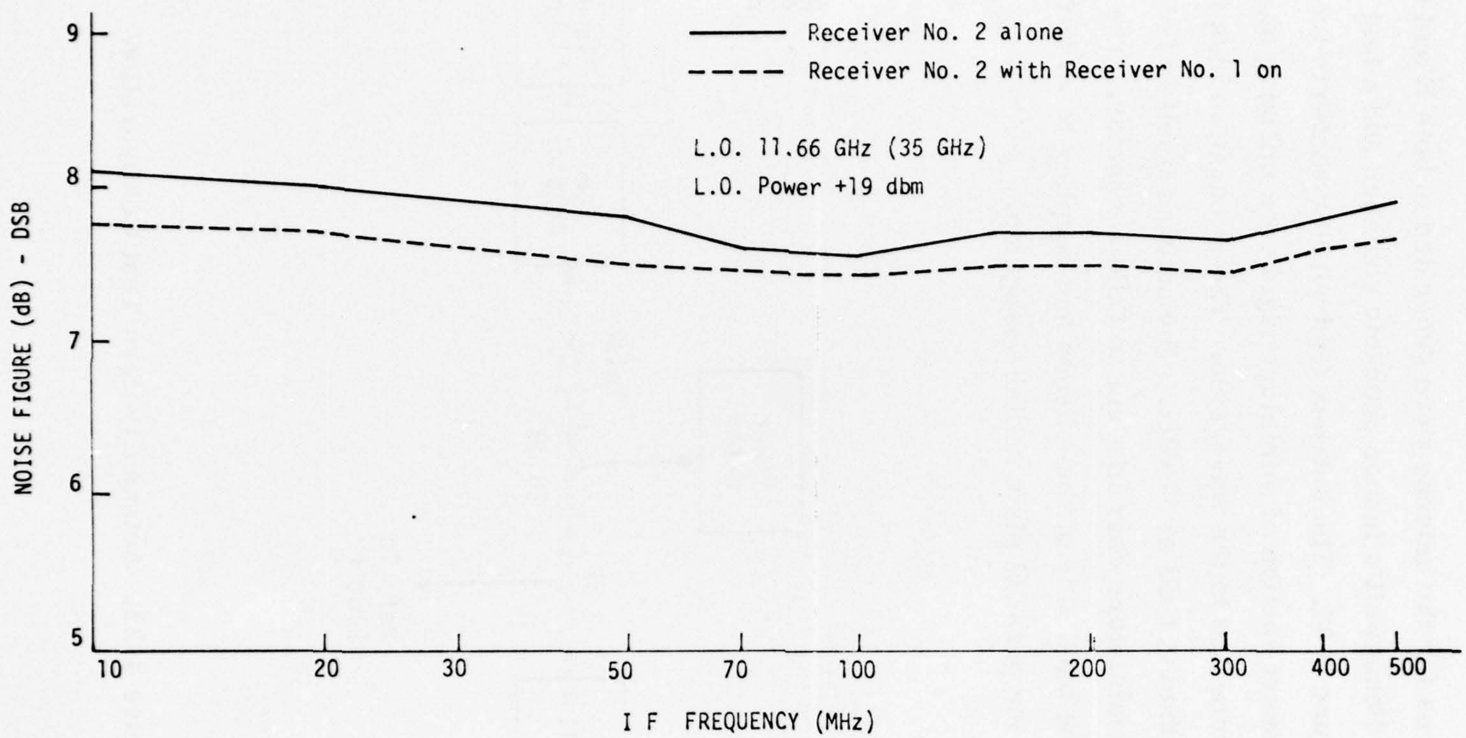

Figure 4-24. Receiver Interaction on Noise Figure
Receiver No. 2

Radiation patterns for the antenna were generated in both E and H planes at 35.4 GHz using Honeywell's indoor anechoic chamber and a test configuration as shown in Figure 4-25. The antenna feed adaptor converts from RG-96 waveguide to a short section of miniature rigid coax utilizing an E-field coupling probe mounted in the waveguide. The attenuation loss in the feed adaptor is less than 0.1 dB at 35 GHz. The antenna itself is fed at its center from the miniature coax line via an OSM connector. The connector is mounted on the back side of the antenna and coupling to an E-field probe at the center of the parallel plate radial waveguide.

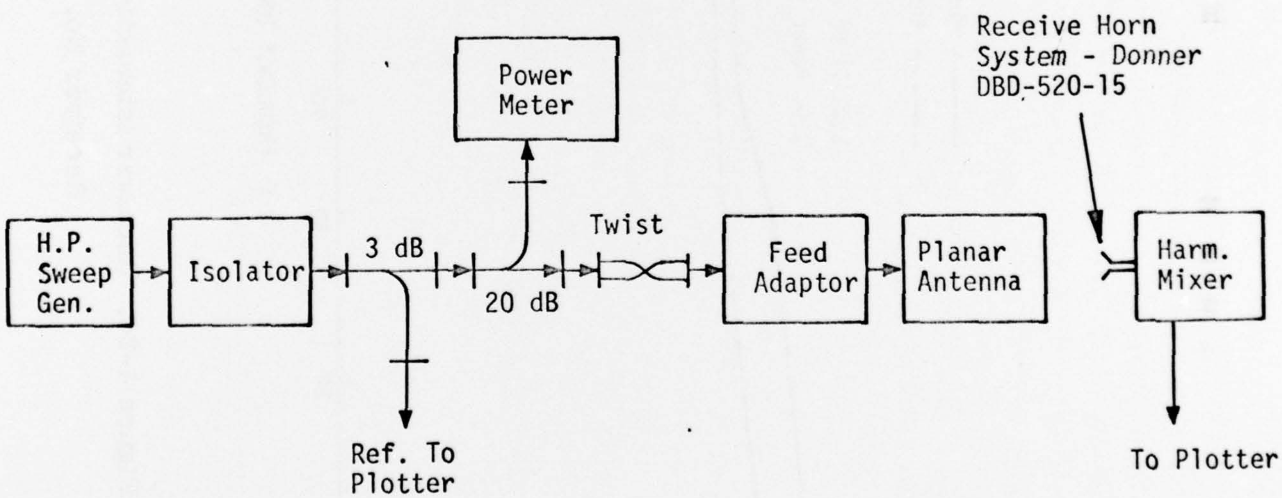

Figure 4-25. Antenna Pattern Test Configuration

Un-normalized radiation patterns are presented in Figures 4-26 and 4-27 for the E and H planes, respectively. The 3 dB beamwidth of the main lobe is approximately 4° in both E and H planes. At present the sidelobe levels are suppressed by only about 10 dB, and efforts are underway to further suppress sidelobes to achieve a design goal of 20 dB or more. An explanation of the apparent non-symmetry in the E-plane pattern can be made in terms of a possible misalignment between the actual E-plane of the antenna and the experimental rotation plane.

Antenna efficiency was roughly estimated by comparing main beam gain with that of a reference horn antenna possessing 24.7 dB of gain at 35.4 GHz (normalized to isotropic). The reference horn was a Scientific Atlanta Model No. 12A-26 antenna with a 3 dB beamwidth of 9° in the E-plane and 10° in the H-plane. The efficiency of the reference horn was nominally 50 percent.

In comparing main beam levels between antennas, losses associated with planar antenna feed adaptor must be separated from those of the antenna itself. In order to do this the reflective and transmission losses of the feed adaptor were measured and found to be on the order of 0.1 dB. The power distribution for both the reference and test antenna systems are shown in Figure 4-28. By using the test configuration illustrated in Figure 4-25 and by interchanging the reference horn with the planar antenna/adaptor unit, it was determined that the main beam gain of the planar antenna (with feed adaptor) was approximately 8 dB less than the main beam gain of the reference antenna.

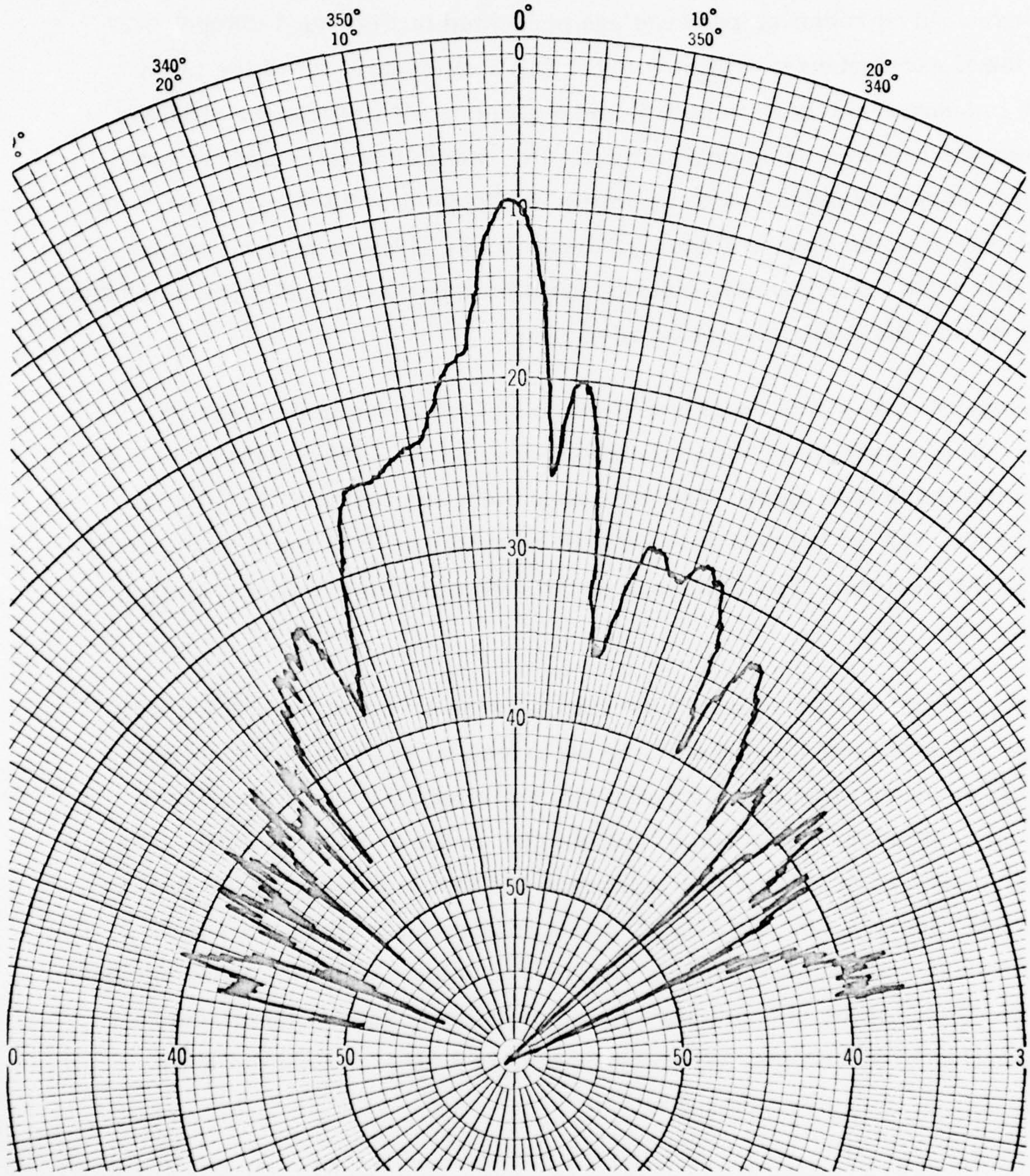

Figure 4-26. E-Plane Radiation Pattern (Un-normalized)
Antenna RA-2 f = 35.4 GHz

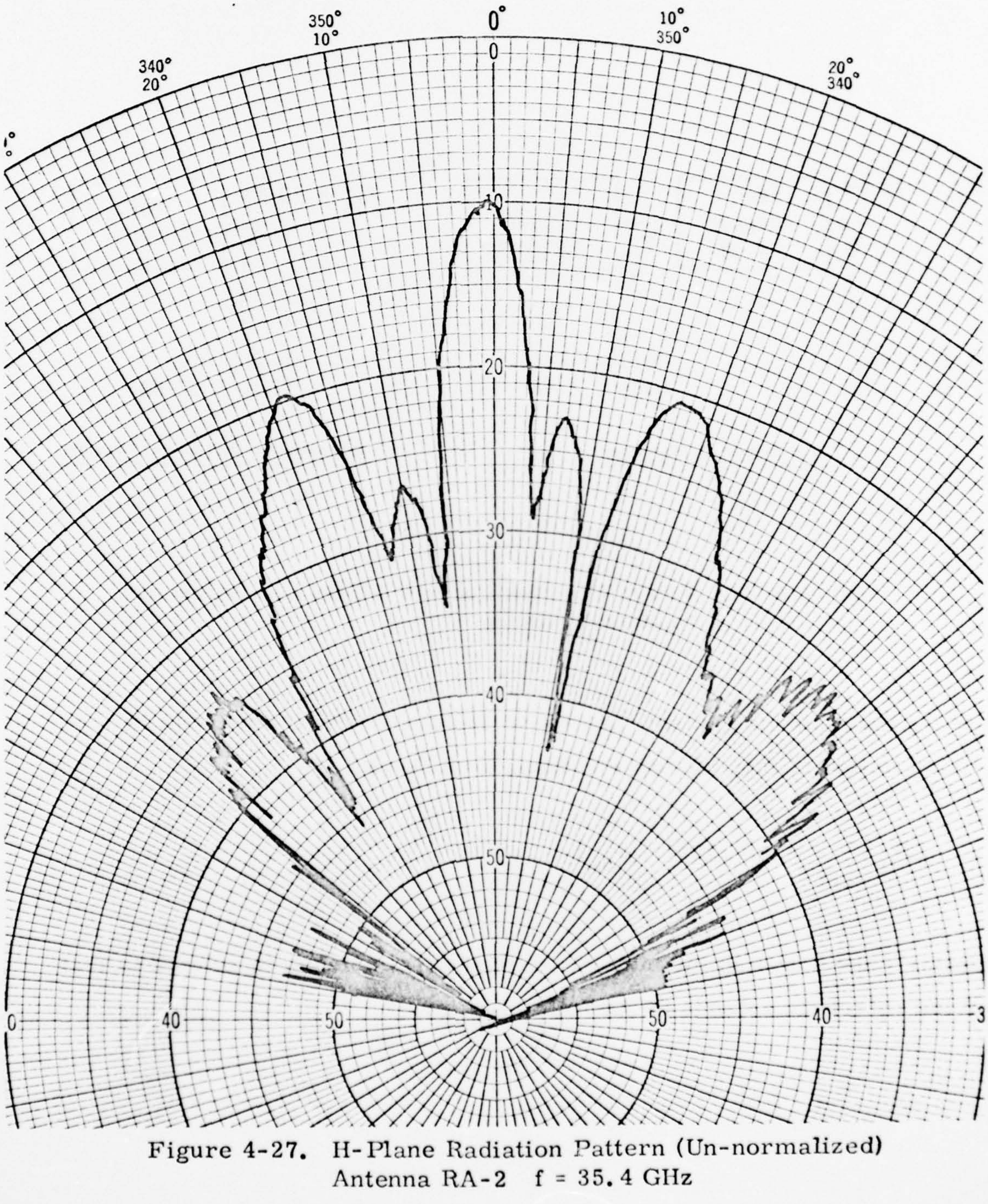

Figure 4-27. H-Plane Radiation Pattern (Un-normalized)
Antenna RA-2 f = 35.4 GHz

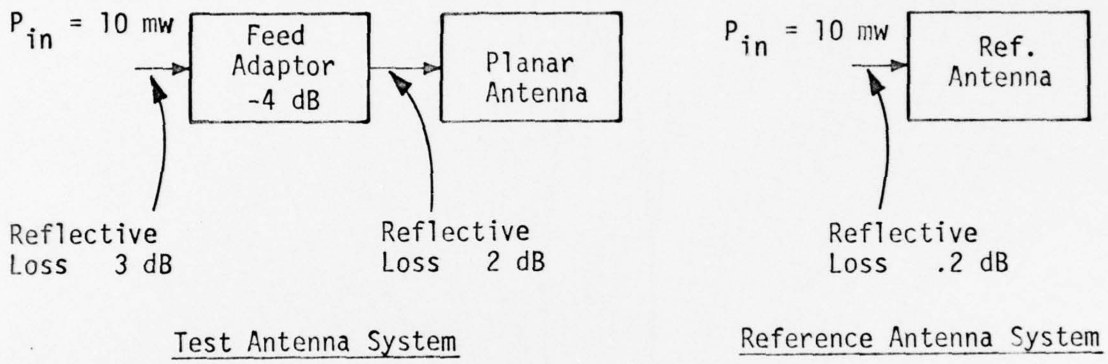

Figure 4-28. Power Distribution in the Test and Reference Antenna Systems

For the test antenna system, the actual input power to the antenna is related to that of the reference antenna as follows:

$$[P_{in}]_{test} = [0.125]\ [P_{in}]_{ref} .$$

Similarly the power in the main beam of the test antenna is related to that for the reference antenna in the following way:

$$[\text{main beam power}]_{test} = [0.158] \frac{\left[\begin{matrix}\text{main}\\ \text{beamwidth}\end{matrix}\right]^2_{test}}{\left[\begin{matrix}\text{main}\\ \text{beamwidth}\end{matrix}\right]^2_{ref}} [\text{main beam power}]_{ref}$$

$$= [0.158] \quad [0.197] \quad [\text{main beam power}]_{ref}$$

$$= (0.031) \quad [\text{main beam power}]_{ref}$$

Using the approximate relationships, the relative efficiency of the planar antenna can be estimated as follows:

$$\eta_{test} \simeq \frac{[\text{main beam power}]_{test}}{[P_{in}]_{test}}$$

$$\simeq [0.25] \; \eta_{ref}$$

Using the efficiency value of 0.5 for the reference horn, the efficiency of the planar antenna tested is crudely estimated to be about 12 percent. This will certainly be a lower bound on actual value of efficiency since the rather significant sidelobes of the test antenna were not included in the estimate. A more detailed evaluation is currently underway to establish efficiency. In addition modifications in dielectric material, resonator, and slot radiator designs are being undertaken to further minimize losses in the antenna.